The American Journal of Human Genetics

Supplemental Data

Concurrent Whole-Genome Haplotyping and Copy-Number Profiling of Single Cells

Masoud Zamani Esteki, Eftychia Dimitriadou, Ligia Mateiu, Cindy Melotte, Niels Van der Aa, Parveen Kumar, Rakhi Das, Koen Theunis, Jiqiu Cheng, Eric Legius, Yves Moreau, Sophie Debrock, Thomas D'Hooghe, Pieter Verdyck, Martine De Rycke, Karen Sermon, Joris R. Vermeesch, and Thierry Voet

Supplemental Note

Single-cell genotyping: evaluation of WGA-methods, SNP-array platforms and genotyping algorithms

We evaluated different WGA-methods in combination with different SNP-typing chemistries (Illumina 300K HumanCytoSNP-12 and Affymetrix 250K NspI SNP-arrays) and conceptually different genotyping algorithms (**Figures S3** and **S4**, **Material and Methods**). User-definable parameters for single-cell genotyping were calibrated using the genotypes derived from multi-cell non-WGA DNA-samples as references (**Figure S4**).

Twelve single cells were harvested from two EBV-transformed lymphoblastoid cell lines, which were derived from two different individuals, "S1" and "S2" respectively, shown in the pedigree in the figure S3. Of each cell line, six single cells were whole-genome amplified by either multiple displacement amplification (MDA; n=3) or the PCR-based PicoPlex (n=3) technology to deliver enough input material for both massively parallel SNP-typing chemistries. Importantly, different algorithms that interpreted the same raw SNP-array data could produce significantly different accuracies of the heterozygous single-cell SNPs when compared to the genotype of the multi-cell non-WGA DNA-sample (**Figure S4**). Furthermore, it was clear that genotypes of MDAed single cells outperformed the genotypes of PicoPlex-WGAed cells with each genotyping platform and algorithm tested. PicoPlex-WGAed cells were characterized by a significantly reduced call rate (e.g. 37.82% ± s.d. 4.43% versus 63.01% ± s.d. 3.92% following Illumina-GenCall genotyping) and a significantly lower accuracy of heterozygous SNP-calls in the cell (e.g. 78.90% ± s.d. 3.17% versus 96.55% ± s.d. 3.02% following Illumina-GenCall genotyping; **Figure S4**). Similar results were obtained with the Affymetrix SNP-typing chemistry (**Figure S4**). Based on overall performance, GenCall genotyping of single-cell WGA products hybridized on Illumina HumanCytoSNP arrays was applied in all downstream analyses, with MDA as the preferred single-cell WGA-method. We furthermore reduced the time-frame of the Illumina protocol from the conventional 3-day to a 24-hour protocol for single-cell genotyping with retaining SNP-typing accuracy following

GenCall (P-values > 0.05, **Figures S3B** and **S4C**, **Material and Methods**). This opens routes for the technology to be applied in clinical practice.

Single-cell data quality control (QC) metrics

A matching accurate multi-cell derived SNP genotype is often lacking for QC-analysis of a single cell's SNP-genotype(s). We investigated whether parental SNP-calls, which are determined from blood-extracted multi-cell DNA samples and which are not necessarily informative for downstream single-cell haplotyping, could be solicited for QC-analysis of a cell's genotype. Indeed, a SNP with paternal AA and maternal BB genotypes is uninformative for haplotyping a diploid cell of a conceptus derived from that couple, but can be instructive in determining ADO events and rates. Similarly, a SNP with paternal BB and maternal BB genotypes (**Material and Methods**) is ineffective for haplotyping, but is informative for determining putative allele drop-in (ADI) events and rates. The latter can arise due to WGA base-copy errors, *in silico* misinterpretation by the genotyping algorithm (**Figure S4C**), or worst-case scenario due to the presence of contaminating DNA in the WGA-reaction as well as sample mix-up. To further control for kinship as well as large-scale DNA copy number aberrations, these concepts were integrated with unsupervised hierarchical clustering of the single-cell genotypes (**Figure S3B**).

As a control, the application of this genotype QC-metric successfully identified cells amplified by PicoPlex to be significantly distinct from cells amplified by MDA (**Figure S3B**). Furthermore, it effectively identified lymphoblastoid cells "S1-ebv03-mda" and "S2-ebv12-picoplex" to have genotypes that are (a) significantly different from the other MDAed and PicoPlex-WGAed cells respectively, and (b) of poor quality due to SNP Mendelian inaccuracies (increased ADO and/or ADI frequencies likely acquired during WGA) with or without decreased genome coverage (i.e. decreased SNP-call rate; **Figure S3B**). Genotypes with such features may lead to inaccurate and non-reliable haplotypes downstream.

Additionally, apart from poor genotypes, substandard single-cell WGA products are usually also characterized by high standard deviations (SD) of the logR values. Since chromosome instability (CIN)

can inflate a cell's genome-wide SD, we developed a cumulative chromosome-specific SD (CSD) metric that allows identifying substandard WGA products from a logR perspective (**Figures S3C**, **D**, **Material and Methods**). In the batch of single-cell MDA samples, cell "S1-ebv03-mda" was detected as an outlier, while in the batch of PicoPlex-amplified cells, cell "S2-ebv12-picoplex" along with three other cells demonstrated higher CSD values (**Figure S3C**).

In general, QC-passed PicoPlex WGAed cells showed consistently higher ADI- and CSD-rates, but lower ADO-rates than QC-passed MDAed cells as well as less genome coverage (**Figure S3B**).

The SNP-data derived from 89 single blastomeres amplified by MDA were first QC-filtered before initiating single-cell haplotyping and copy number typing. Twenty-nine blastomeres did not pass these stringent QC-metrics: 24 out of 89 (27%) single blastomeres were filtered by the CSD-metric (**Figure S8**); 5 (6%) by the genotype metric (**Figure S8**). Besides technical noise in the logR-values, the CSD-metric can also detect biological noise resulting from the cell cycle. Indeed, cells in S-phase of the cell cycle will generate oscillated logR patterns[1] reflecting early and late replication domains. Similar QC-rates have been reported in other studies; albeit different cell types, WGA-methods and platforms (aCGH [2], SNP-array [2; 3] and next-generation sequencing [3; 4]) were applied in those studies.

Validation of siCHILD for single-cell haplotyping using preimplantation genetic diagnosis

For families PGD002, PGD004, PGD005, PGD006, PGD008, PGD012, PGD018 and PGD020 an affected sibling's genotype was used as a seed for parental allelic phasing, while in families PGD014, PGD016 and PGD022 a grandparental genotype was applied. For family PGD021, both affected sibling and grandparental genotypes were available as seeds for parental phasing. The accuracy of siCHILD was proven by validating the detection of haplotypes that carry disease variants, with standard PCR- or FISH-based (PGD) assays on the same embryo. All siCHILD-results were proven accurate; further proving that

with current amount of measurements (n=62), we have 95% statistical confidence that fewer than 5% of tests may produce a discrepant result (**Material and Methods**).

Single-cell haplotyping by siCHILD enables generic PGD for autosomal and X-linked Mendelian disorders

In PGD014, the segregation of a 1.4 Mb duplication of the peripheral myelin protein 22 gene (*PMP22*) causing the autosomal dominant demyelinating neuropathy type 1 Charcot-Marie Tooth disease (OMIM 118220) was tracked from an affected father to three IVF-embryos using siCHILD single-cell haplotyping. Two blastomeres per embryo (n=3) were characterized. All blastomeres carried the affected paternal haplotype at the 17p11.2 locus, but one blastomere (Bl522 of embryo E02) had lost a large part of the paternal allele of chromosome 17, while another blastomere (Bl520 of embryo E01) carried a trisomy 17 consisting of two affected paternal alleles and one normal maternal allele (**Table S7**). The traditional PCR-based PGD of two separate blastomeres from each embryo was consistent with these results (**Table S7**).

Family PGD021 is at risk for both the autosomal recessive cystic fibrosis (OMIM 219700) as well as the autosomal dominant Diamond-Blackfan anemia condition (OMIM 105650). Both parents are carrying a mutant *CFTR* gene, while only the father carries the Diamond-Blackfan anemia causing *RPS19* mutation. Amongst the three biopsied IVF-embryos, siCHILD found one embryo (E10 in **Table S7**) to be free of the *CFTR* mutant alleles but carrying the paternal *RPS19* mutant allele, one embryo (E05 in **Table S7**) to be carrying a maternal *CFTR* mutant allele as well as the paternal *RPS19* mutant allele, and one embryo to be carrying the maternal and paternal *CFTR* mutant alleles but to be free of the paternal *RPS19* mutant allele (E14 in **Table S7**). All results were concordant with the traditional PCR-based PGD (**Table S7**).

In PGD020, a single blastomere of one IVF-embryo was tested with siCHILD for the inheritance of the mutated *CFTR* alleles present in both parents. A monosomy 7 was detected, with the remaining paternal chromosome carrying the non-mutated *CFTR* allele. This confirmed the PCR-based PGD.

In PGD006, the father is affected with a 17q24.2 deletion syndrome. Three blastomeres derived from two embryos were analyzed. One embryo was diagnosed as a non-carrier (E10 in **Table S7**), while the other was diagnosed as affected (E12 in **Table S7**) using siCHILD. This confirmed the FISH-PGD results obtained for both embryos (**Table S7**).

PGD018 for OMIM 603903 is described in the main text, as are all cases at risk for an X-linked recessive disorder (PGD005 for a microdeletion Xp22.31 syndrome; PGD012 for hemophilia A; PGD016 for Duchenne Muscular Dystrophy; PGD022 for Fragile X syndrome).

Single-cell haplotyping by siCHILD enables generic PGD for simple and complex translocations

PGD004 having a paternal t(1;16)(p36;p12) is described in the main text.

In PGD002, a non-carrier embryo was diagnosed following siCHILD analysis, which confirmed the FISH-based PGD of another cell biopsied earlier from the same embryo (**Table S9**: PGD002 – E02).

For PGD008 burdened with a maternal complex chromosomal rearrangement (CCR) t(6;13;16)(p25.1;q21.33;q24.2), we profiled 11 blastomeres from 9 embryos (**Table S10**). Similar to the approach described in the main text for simple reciprocal translocations, the inheritance of the normal and derivative chromosomes could be discerned by tracking the inheritance of the haplotypes flanking the translocation breakpoints. In one embryo, the presence of the 3 derivative chromosomes was detected which resulted in the inheritance of a balanced maternal complement involving chromosomes der(6),

der(13) and der(16) (**Table S10** – Embryo E11), while no conclusive FISH-based PGD result had been obtained of a sister blastomere biopsied from the same embryo. In six other embryos, siCHILD haplotype analysis indicated the presence of various combinations of derivative and normal chromosomes per cell, predicting the inheritance of unbalanced maternal chromosome configurations (**Table S10** – Embryos E06, E09, E10, E14 and E15 from cycle 1, and embryo E05 from cycle 2). For five of the six embryos, a conclusive FISH-based PGD of a sister blastomere biopsied from the same embryo could be obtained, while the sister blastomere from the remaining embryo displayed no interpretable FISH results during the conventional PGD. The conclusive FISH results corroborated siCHILD's diagnosis, although mosaicism in cleavage stage embryogenesis was evident for one embryo (**Table S10** – Embryo E09). Two blastomeres of two embryos demonstrated missing maternal chromosomes involved in the CCR (**Figure 7**, **Table S10** – Embryos E08 and E11 from cycle 1). One blastomere could not be diagnosed by siCHILD due to homologous recombination sites very near to the regions of interest (**Table S10** – Embryo E03 from cycle 2).

Figure S1

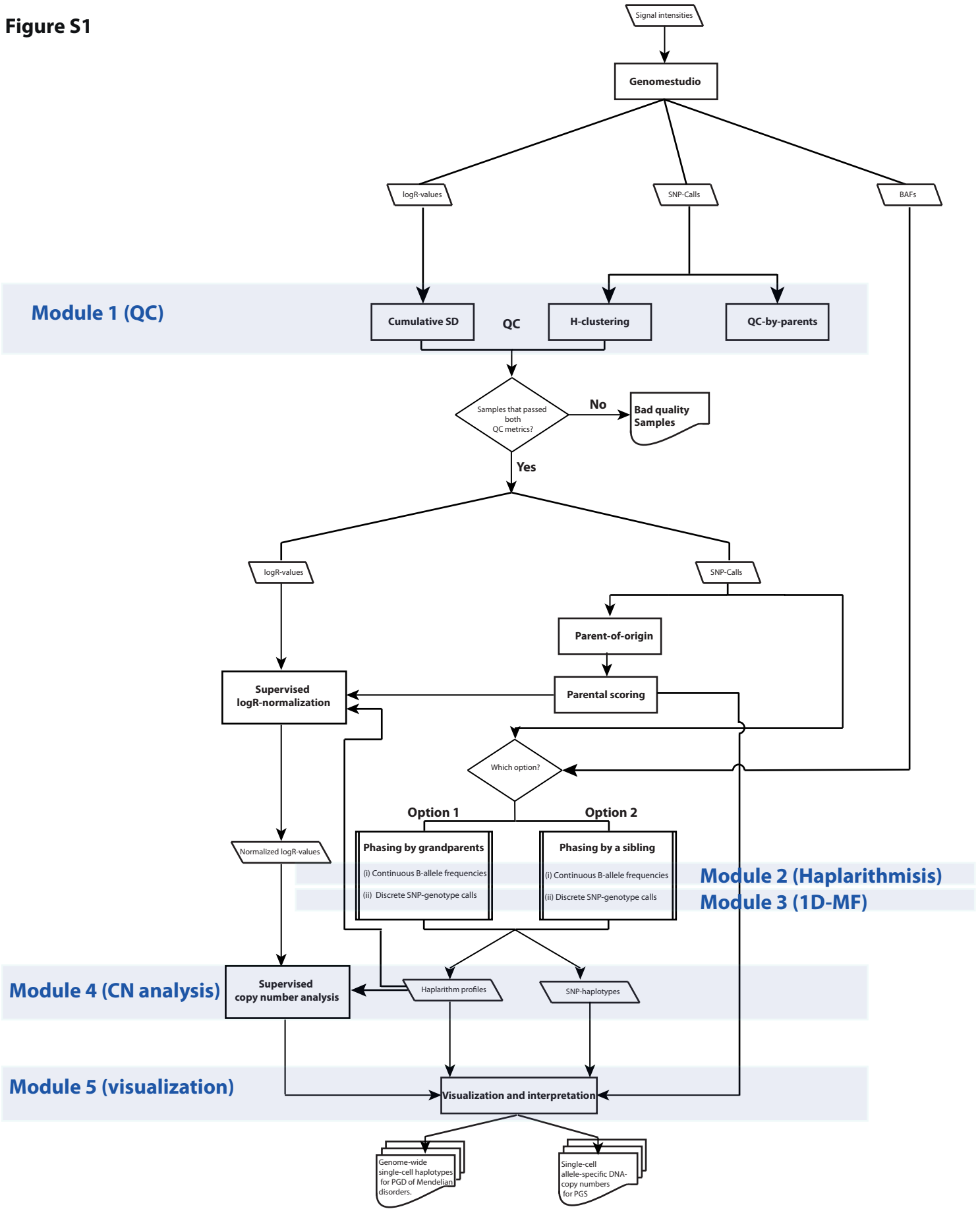

Figure S1 | Overview of the siCHILD algorithm. Single-cell SNP-logR values and discrete SNP-genotype calls following SNP-data extraction with Genomestudio are applied for QC-analysis. Substandard single-cell SNP-array data are filtered out. The single-cell SNP-genotypes are haplotyped using the parental genotypes, which are in turn phased by using the genotypes of either a sibling or a grandparent as a seed. These primary haplotypes are converted by 1D median filtering to the single-cell haplotype blocks. The single-cell haplotype blocks are independently confirmed with haplarithmisis. Finally, haplarithmisis is applied for logR-value normalization and supervised copy-number analysis.

Figure S2

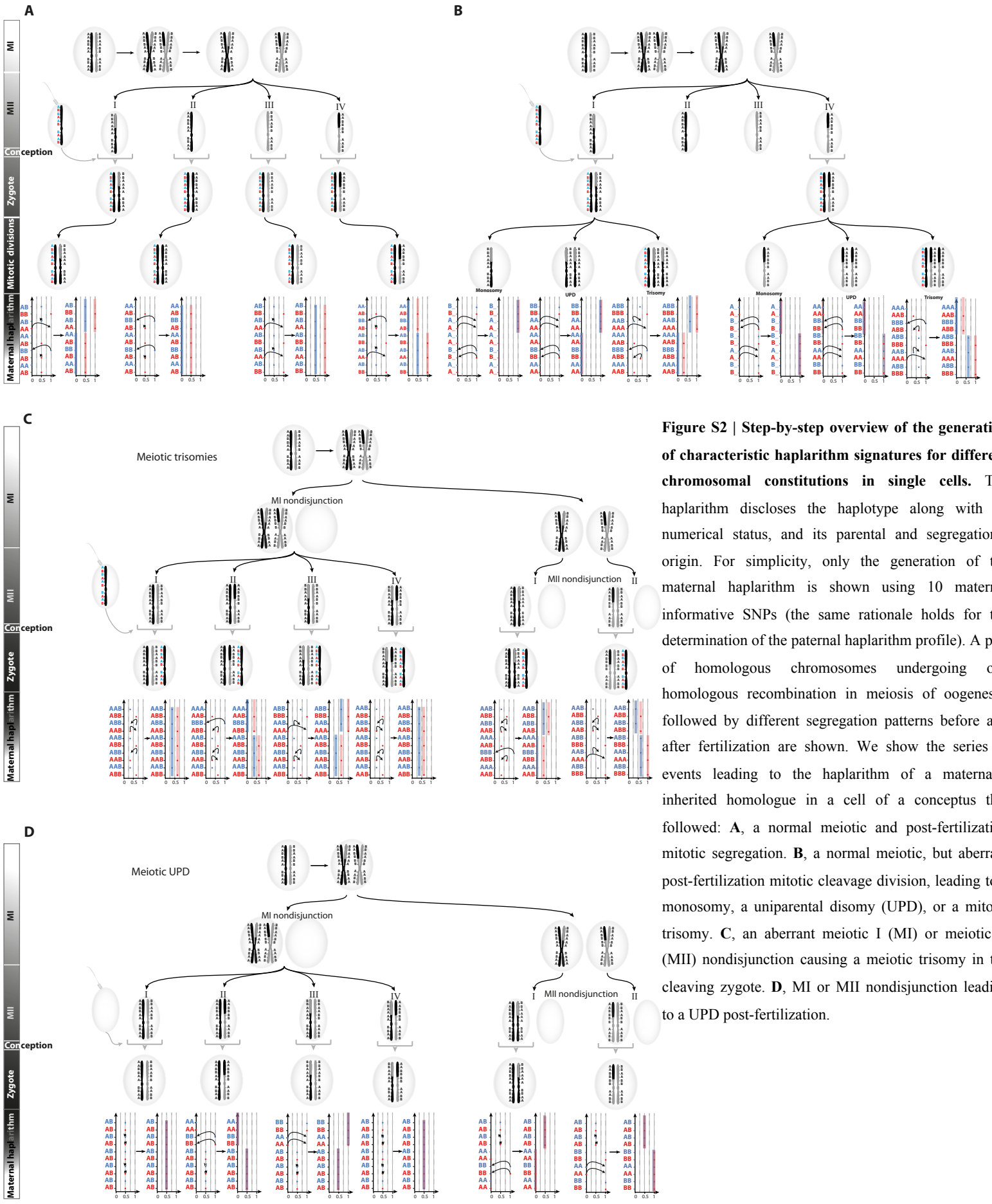

Figure S2 | Step-by-step overview of the generation of characteristic haplarithm signatures for different chromosomal constitutions in single cells. The haplarithm discloses the haplotype along with its numerical status, and its parental and segregational origin. For simplicity, only the generation of the maternal haplarithm is shown using 10 maternal informative SNPs (the same rationale holds for the determination of the paternal haplarithm profile). A pair of homologous chromosomes undergoing one homologous recombination in meiosis of oogenesis, followed by different segregation patterns before and after fertilization are shown. We show the series of events leading to the haplarithm of a maternally inherited homologue in a cell of a conceptus that followed: **A**, a normal meiotic and post-fertilization mitotic segregation. **B**, a normal meiotic, but aberrant post-fertilization mitotic cleavage division, leading to a monosomy, a uniparental disomy (UPD), or a mitotic trisomy. **C**, an aberrant meiotic I (MI) or meiotic II (MII) nondisjunction causing a meiotic trisomy in the cleaving zygote. **D**, MI or MII nondisjunction leading to a UPD post-fertilization.

Figure S3

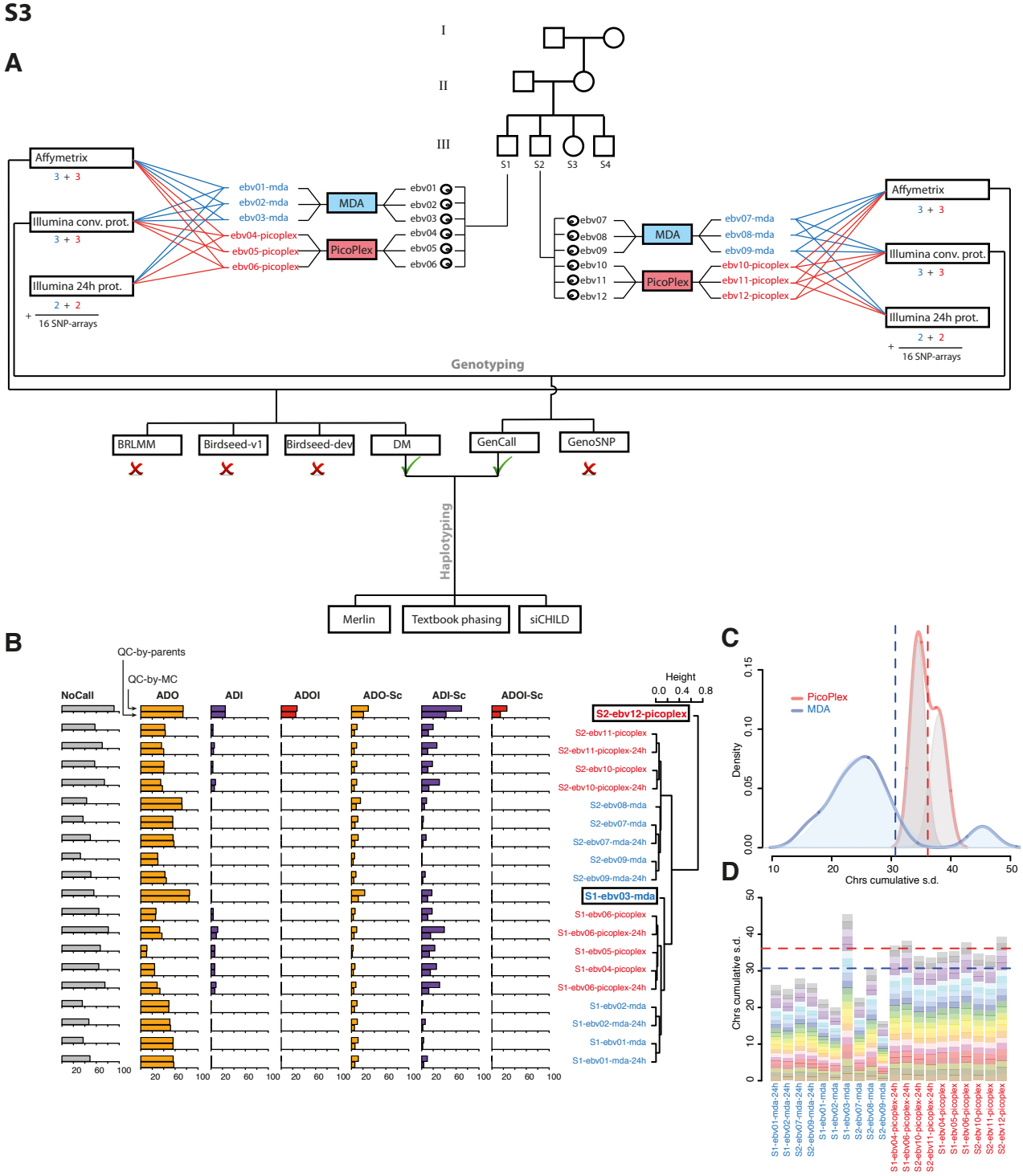

Figure S3 | Development of single-cell SNP-typing and data QC-metrics using the EBV-transformed lymphoblastoid cells. A, Flowchart of the optimization of single-cell genotyping using Affymetrix and Illumina SNP-arrays. Of EBV-transformed lymphoblastoid cell lines derived from two individuals 'S1' and 'S2', six single cells per individual were isolated of which three were whole-genome amplified using MDA and three using PicoPlex. These WGA-products were hybridized to Affymetrix NspI 250K SNP-arrays as well as to Illumina HumanCytoSNP-12 SNP-arrays following the protocol as recommended by the company. Four single-cell WGA-products of each individual were also hybridized to the Illumina SNP-arrays following a rapid-mode protocol (**Material and Methods**). Subsequently, the SNP-probe signals were interpreted by different genotyping algorithms. Based on overall performance (**Figure S4**), we decided to use GenCall for interpreting Illumina SNP-probe signals, and the Dynamic Model (DM) for interpreting Affymetrix SNP-probe signals of single cells. **B**, QC metrics applied on the GenCall SNP genotypes of single cells. To compute ADO, ADI, ADOI, we used the matching multi-cell DNA sample as a reference [indicated with QC-by-MC]. For ADO-sc, ADI-sc and ADOI-sc computation (**Material and Methods**), we used the SNP-genotypes of the parents as a reference of expected genotypes [indicated with QC-by-parents]. Single-cell genotypes were in addition subjected to hierarchical clustering for QC-analysis. Samples S1-ebv03-MDA and S2-ebv12-PicoPlex can be noted as clear outliers. Furthermore, PicoPlex-WGA led to higher ADI and NoCall rates, but lower ADO rates than single-cell MDA WGA. **C, D**, Cumulative chromosome-specific standard deviation (CSD) as a QC-metric to identify substandard single-cell WGA products on the basis of noise in the logR landscape. The logR values resulting from single-cell Illumina SNP-typing were used. The dashed lines indicate the thresholds applied on the maximum CSD-values following analysis of the density distribution of all single-cell CSD-values (**C**). Stacked CSD-values per cell are also illustrated (**D**).

Figure S4

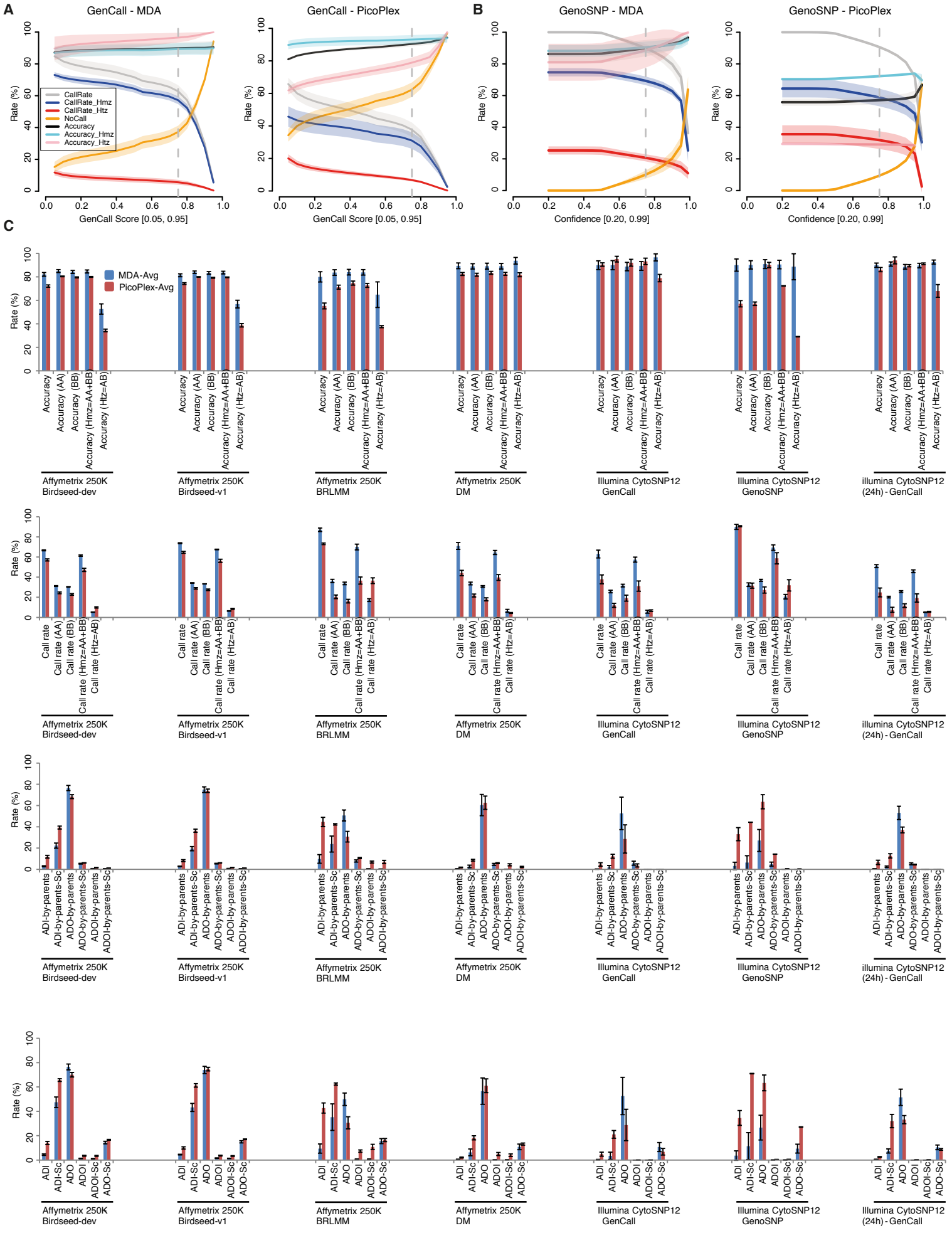
A
GenCall - MDA
GenCall - PicoPlex
B
GenoSNP - MDA
GenoSNP - PicoPlex
Rate (%)
CallRate
CallRate_Hmz
CallRate_Htz
NoCall
Accuracy
Accuracy_Hmz
Accuracy_Htz
GenCall Score [0.05, 0.95]
Confidence [0.20, 0.99]
C
MDA-Avg
PicoPlex-Avg
Accuracy
Accuracy (AA)
Accuracy (BB)
Accuracy (Hmz=AA+BB)
Accuracy (Htz=AB)
Call rate
Call rate (AA)
Call rate (BB)
Call rate (Hmz=AA+BB)
Call rate (Htz=AB)
ADI-by-parents
ADI-by-parents-Sc
ADO-by-parents
ADO-by-parents-Sc
ADOI-by-parents
ADOI-by-parents-Sc
ADI
ADI-Sc
ADO
ADOI
ADOI-Sc
ADO-Sc
Affymetrix 250K Birdseed-dev
Affymetrix 250K Birdseed-v1
Affymetrix 250K BRLMM
Affymetrix 250K DM
Illumina CytoSNP12 GenCall
Illumina CytoSNP12 GenoSNP
illumina CytoSNP12 (24h) - GenCall

Figure S4 | Evaluation of different SNP-typing chemistries, genotyping algorithms and WGA methods for single-cell genotyping. **A**, Determination of algorithmic parameters for optimal single-cell genotyping with the Illumina CytoSNP12 platform. The GenCall score in the genotyping algorithm was varied from 0.05 to 0.95 (X-axis). Subsequently, SNP-call rates were determined, and SNP-call accuracies obtained with single-cell MDA (left panel) and PicoPlex (right panel) WGA products were computed using the genotypes from the matching multi-cell DNA sample as a reference (Y-axis). A GenCall score of 0.75 was chosen as an optimal parameter. Note the differences in heterozygous SNP-calling accuracy between single-cell MDA (left panel) and PicoPlex (right panel) products. A color legend for the different lines is implemented on the panel. The mean accuracy and mean call rates are depicted as lines, the standard deviations as shaded areas surrounding the mean. **B,** Similarly, the GenoSNP confidence parameter was tuned from 0.20 to 0.99 in the algorithm (X-axis). **C,** SNP-call accuracies, call rates, allele drop-out (ADO) rates, allele drop-in (ADI) rates and rates of total allele drop-out complemented with allele drop-in (ADOI) are depicted for single-cell MDA (shown in blue; error bars indicate s.d.) and single-cell PicoPlex (shown in red; error bars indicate s.d.) hybridized on both the Affymetrix NspI 250K SNP-array (genotyped with Birdseed-dev, Birdseed-v1, BRLMM, and DM) and the Illumina CytoSNP12 platform (genotyped with GenCall and GenoSNP). For the latter, the results following both the conventional protocol as recommended by the company as well as following the rapid SNP-typing assay are shown. The rapid protocol retains SNP-typing accuracy following GenCall in comparison with the conventional protocol (P-values > 0.05; Wilcoxon rank-sum test).

Figure S5

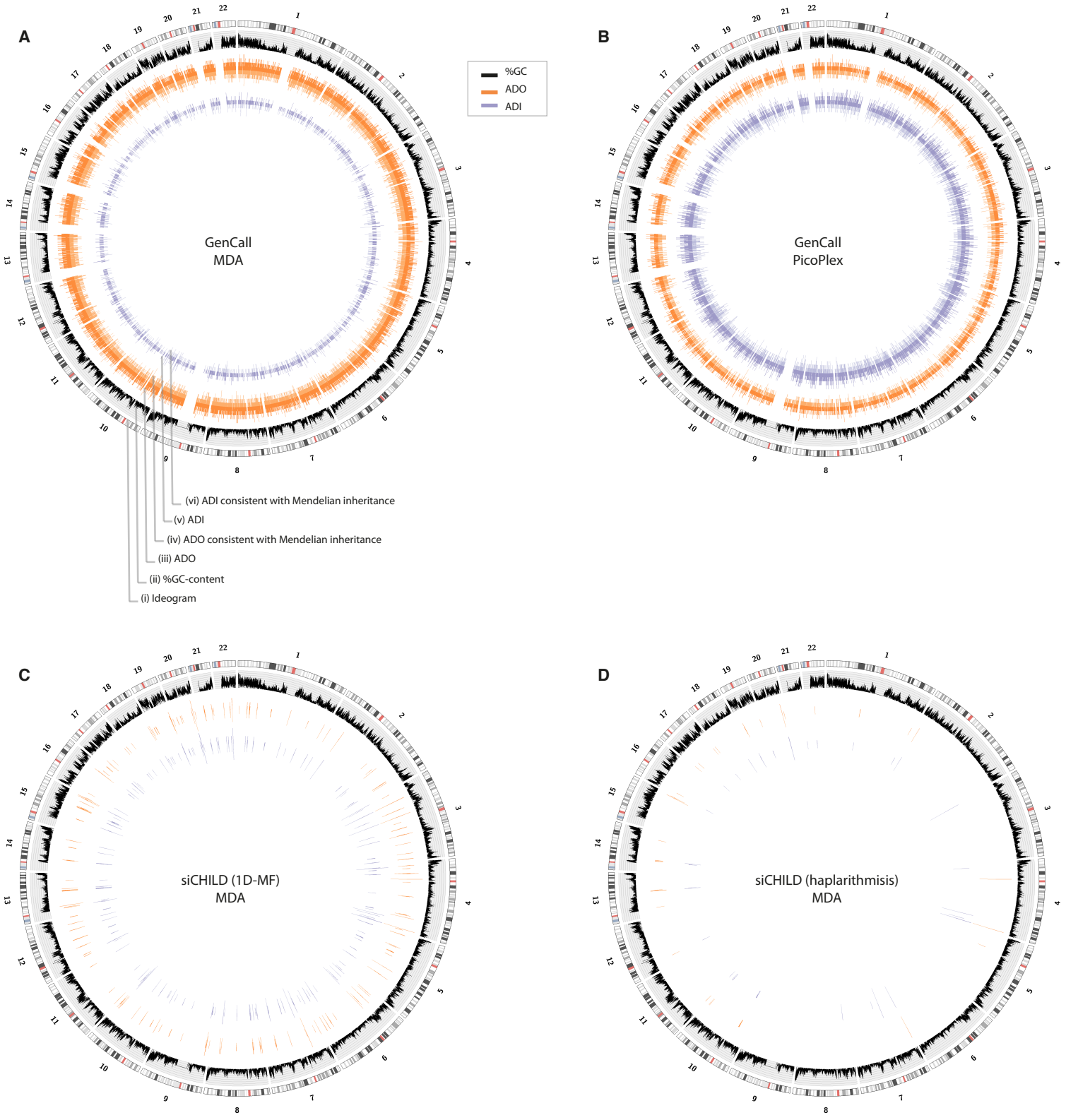

Figure S5 | WGA-induced SNP-call artefacts. A, B, In the Circos plots we show: (i) an ideogram of the autosomes, (ii) local %GC-content of the genome, (iii) ADO events in single-cell genotypes when compared to a multi-cell non-WGA reference genotype, (iv) ADO events in single-cell genotypes when compared to a multi-cell non-WGA reference genotype but which remain consistent with Mendelian inheritance rules, (v) ADI events in single-cell genotypes when compared to a multi-cell non-WGA reference genotype, (vi) ADI events in single-cell genotypes when compared to a multi-cell non-WGA reference genotype which are not in violation with Mendelian inheritance rules. **A**, SNP-call artefacts following single-cell MDA WGA. **B**, SNP-call artefacts following single-cell PicoPlex WGA. **C** SNP-call artefacts following genotype inference from siCHILD 1D-MF haplotypes of single-cell genomes amplified with MDA. **D** SNP-call artefacts following genotype inference from siCHILD haplarithm haplotypes of single-cell genomes amplified with MDA.

Figure S6

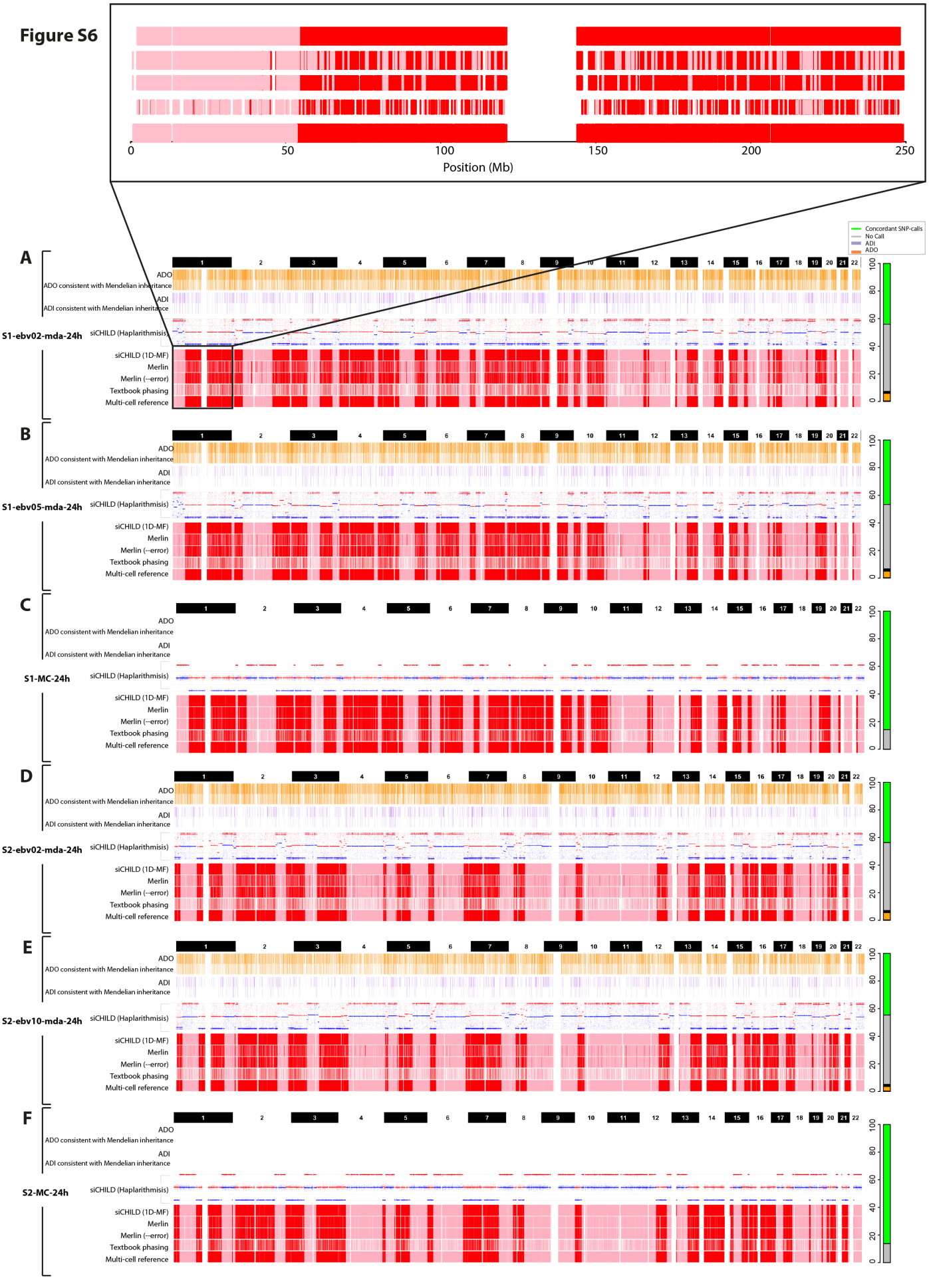
0
50
100
150
200
250
Position (Mb)
Concordant SNP-calls
No Call
ADI
ADO
A
B
C
D
E
F
ADO
ADO consistent with Mendelian inheritance
ADI
ADI consistent with Mendelian inheritance
S1-ebv02-mda-24h
S1-ebv05-mda-24h
S1-MC-24h
S2-ebv02-mda-24h
S2-ebv10-mda-24h
S2-MC-24h
siCHILD (Haplarithmisis)
siCHILD (1D-MF)
Merlin
Merlin (--error)
Textbook phasing
Multi-cell reference

Figure S6 | Comparison of methods for single-cell haplotyping. A-F, We show: (i) an ideogram of the autosomes, (ii) ADO events in single-cell genotypes when compared to a multi-cell non-WGA reference genotype, (iii) ADO events in single-cell genotypes when compared to a multi-cell non-WGA reference genotype but which remain consistent with Mendelian inheritance rules, (iv) ADI events in single-cell genotypes when compared to a multi-cell non-WGA reference genotype, (v) ADI events in single-cell genotypes when compared to a multi-cell non-WGA reference genotype which are not in violation with Mendelian inheritance rules, (vi) the maternal haplarithm from siCHILD, (vii) the maternal 1D-MF haplotypes following siCHILD, (viii) maternal haplotypes determined with Merlin (--best command line option), (ix) maternal haplotypes determined with Merlin (--best command line option, following --error and Pedwipe), (x) maternal haplotypes determined with standard textbook phasing using Mendelian inheritance rules, and (xi) the maternal multi-cell reference haplotype. In the stacked barplot on the right, we show the fractions of SNPs called in the cell (green color bar for SNP-calls concordant with the multi-cell, orange color bar for SNP-calls demonstrating an ADO event, purple color bar for SNP-calls demonstrating an ADI event) and not called (grey color bar). **A**, Data for lymphoblastoid cell S1-ebv02-mda-24h. A zoom-in on the haplotypes of chromosome 1 is provided. **B**, Data for lymphoblastoid cell S1-ebv05-mda-24h. **C**, Data for the multi-cell sample of S1-MC-24h of individual S1. **D**, Data for lymphoblastoid cell S2-ebv02-mda-24h. **E**, Data for lymphoblastoid cell S2-ebv10-mda-24h. **F**, Data for the multi-cell sample of S2-MC-24h of individual S2.

Figure S7

I. Families with an autosomal dominant or recessive disorder

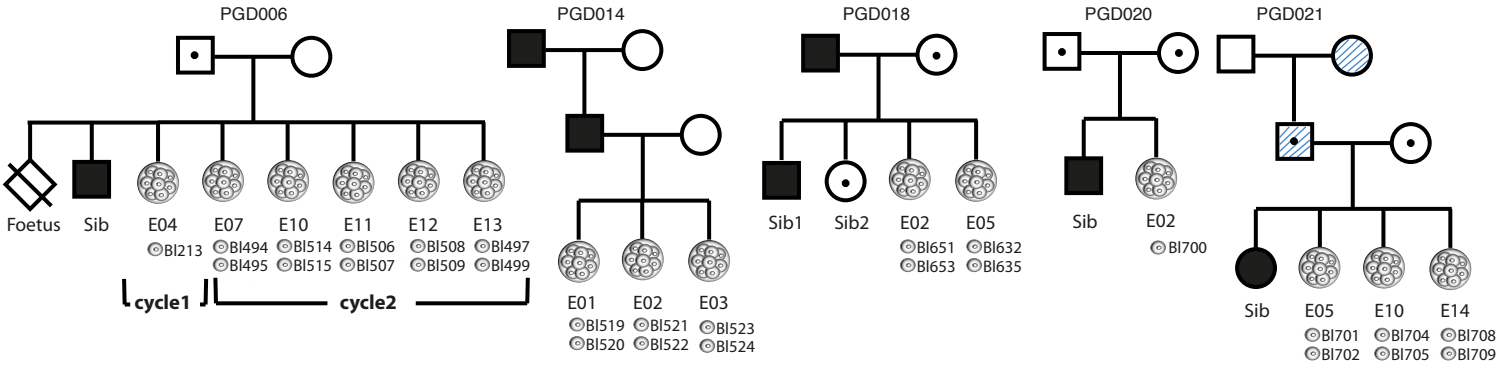

II. Families with an X-linked disorder

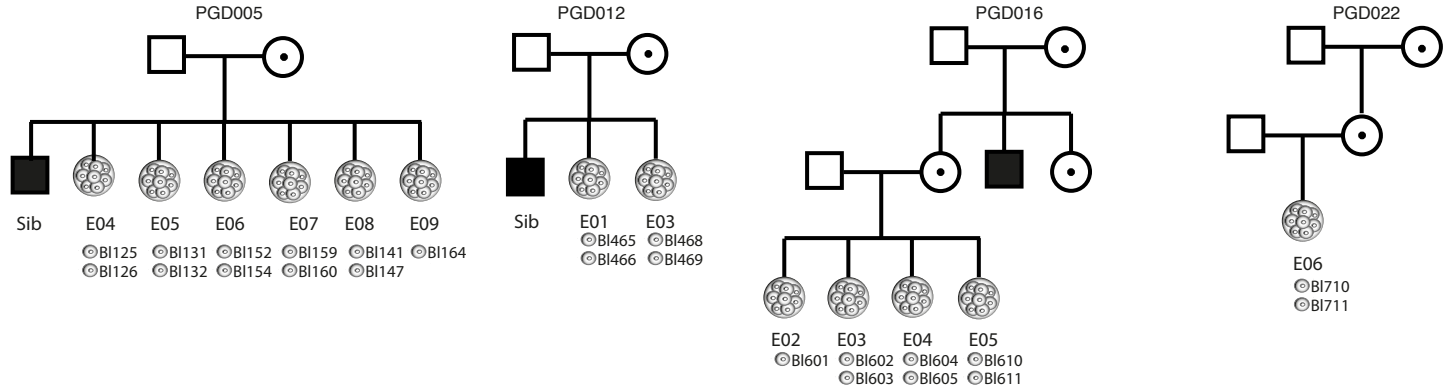

III. Families with a reciprocal translocation carrier

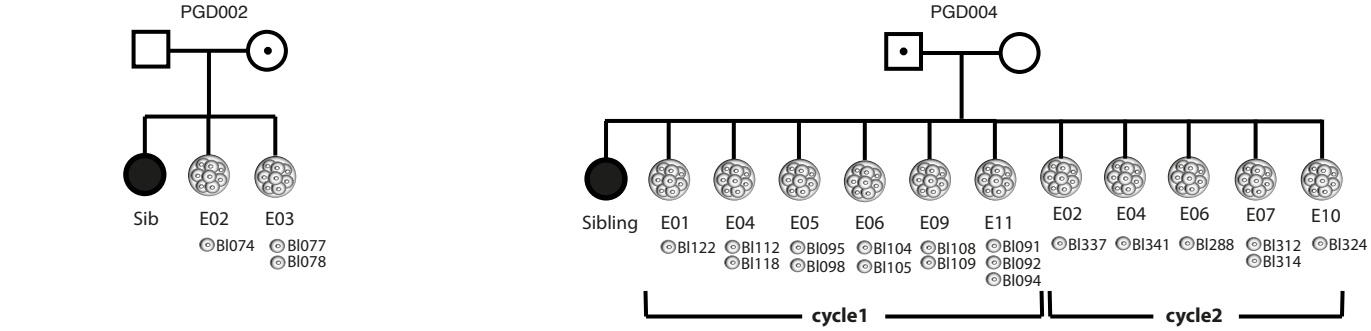

IV. Family with a complex chromosomal rearrangment (three-way CCR)

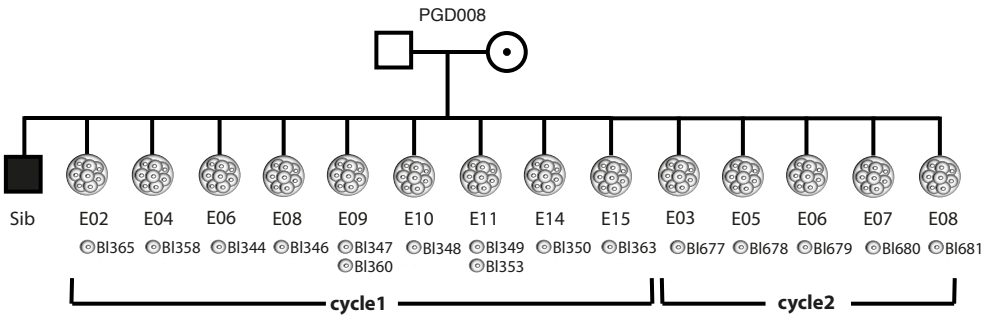

Figure S7 | Pedigrees of the four patient groups that participated in the study. The available family members, the IVF-embryos and SNP-typed blastomeres of each embryo are indicated on the figure.

Figure S8

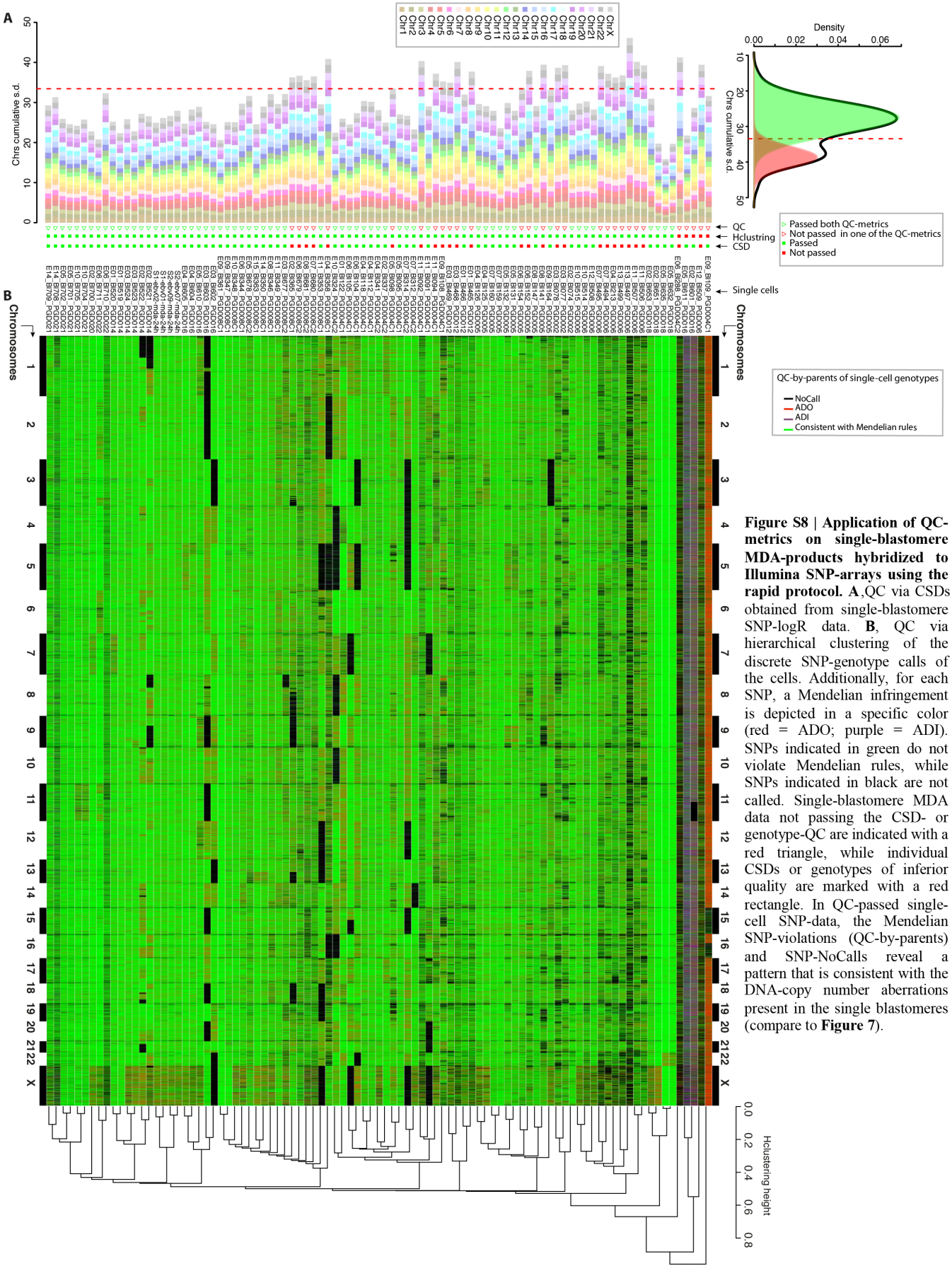

Figure S8 | Application of QC-metrics on single-blastomere MDA-products hybridized to Illumina SNP-arrays using the rapid protocol. A,QC via CSDs obtained from single-blastomere SNP-logR data. **B**, QC via hierarchical clustering of the discrete SNP-genotype calls of the cells. Additionally, for each SNP, a Mendelian infringement is depicted in a specific color (red = ADO; purple = ADI). SNPs indicated in green do not violate Mendelian rules, while SNPs indicated in black are not called. Single-blastomere MDA data not passing the CSD- or genotype-QC are indicated with a red triangle, while individual CSDs or genotypes of inferior quality are marked with a red rectangle. In QC-passed single-cell SNP-data, the Mendelian SNP-violations (QC-by-parents) and SNP-NoCalls reveal a pattern that is consistent with the DNA-copy number aberrations present in the single blastomeres (compare to **Figure 7**).

Figure S9

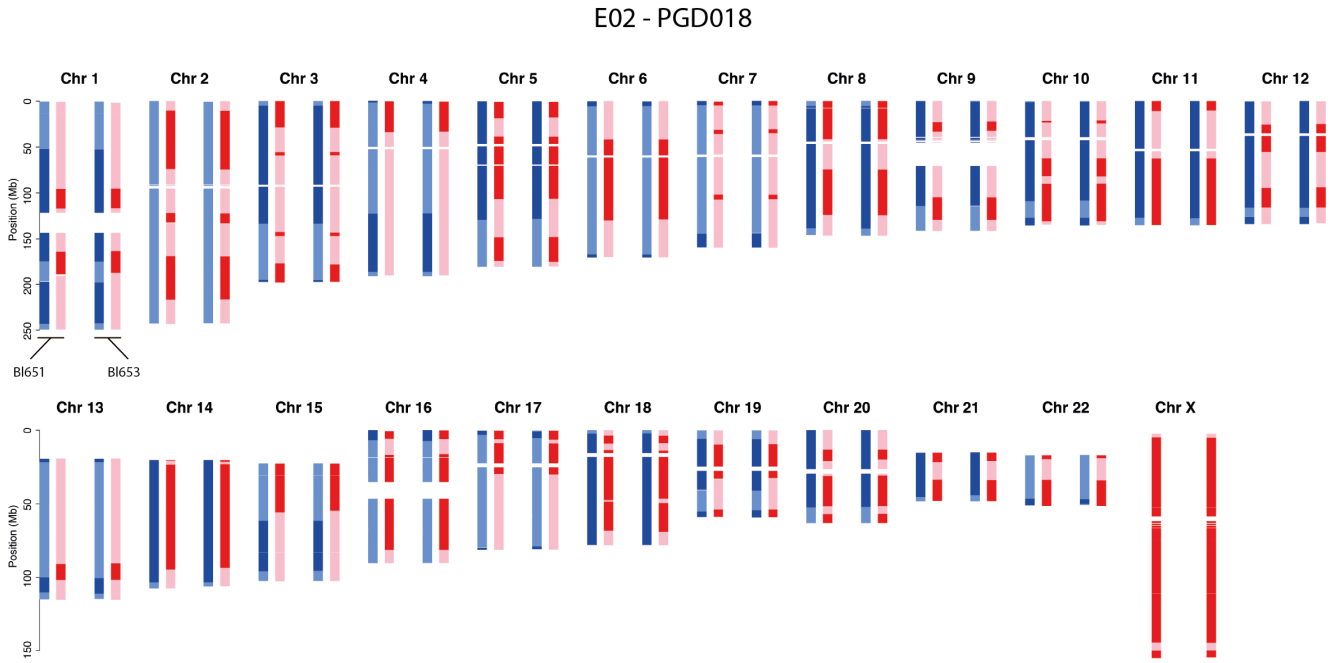

Figure S9 | Reproducibility of siCHILD-determined haplotypes. Paternal and maternal haplotypes of two single blastomeres derived from the same embryo (E02 of PGD018; see also **Table S6**) are shown. Note the high similarity.

Figure S10

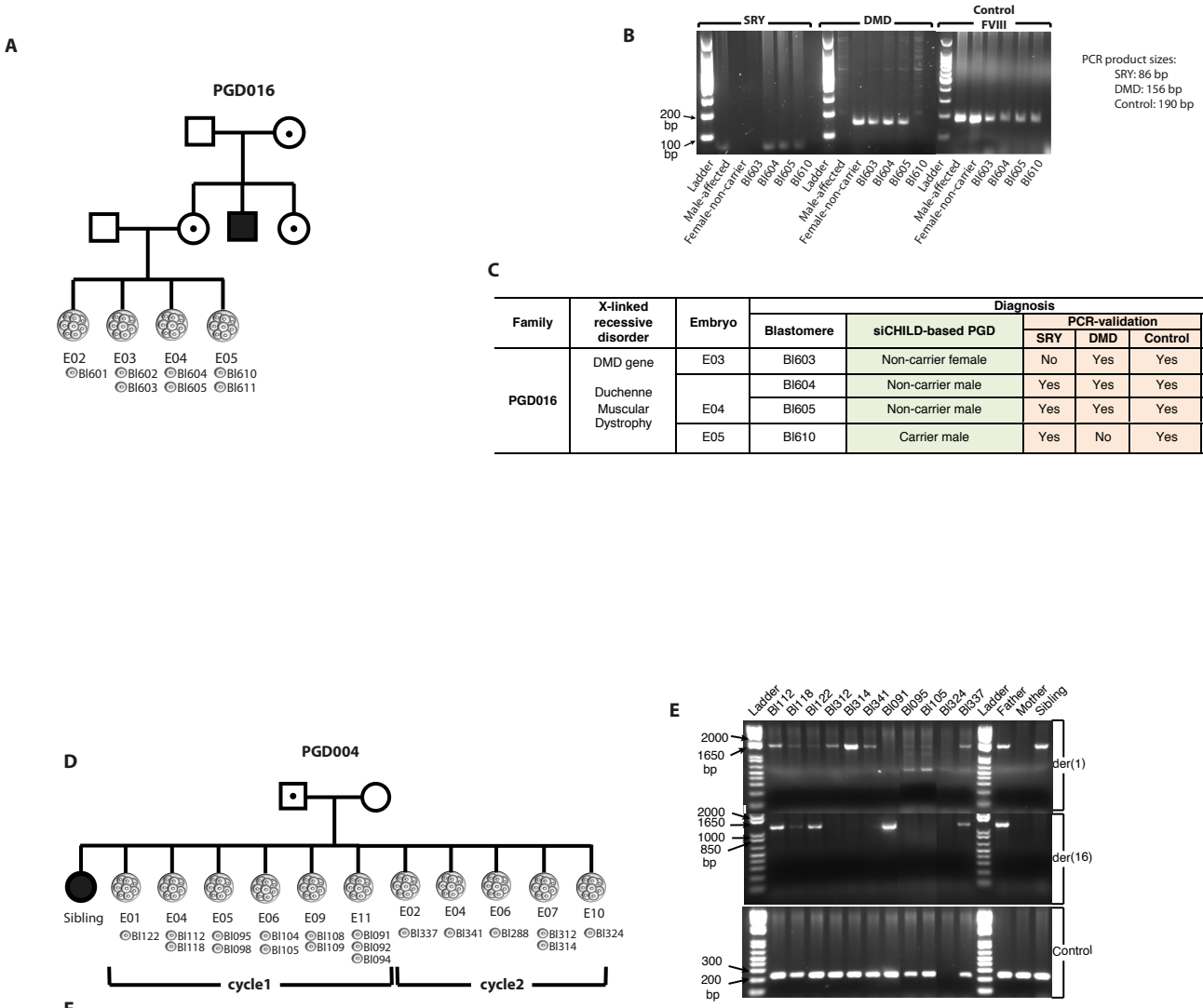

Family	X-linked recessive disorder	Embryo	Diagnosis					
			Blastomere	siCHILD-based PGD	PCR-validation			Concordant
					SRY	DMD	Control	
PGD016	DMD gene Duchenne Muscular Dystrophy	E03	BI603	Non-carrier female	No	Yes	Yes	Yes
		E04	BI604	Non-carrier male	Yes	Yes	Yes	Yes
			BI605	Non-carrier male	Yes	Yes	Yes	Yes
		E05	BI610	Carrier male	Yes	No	Yes	Yes

Family	Translocation	Embryo	Diagnosis							
			Blastomere	siCHILD-based PGD			PCR-validation			Concordant
				Haplotype [a]	Copy number aberration	Segregation	der(1)	der(16)	control	
PGD004	Paternal t(1;16)(p36.33; p12.1) (IVF-cycle 1)	E01	BI122	der(1); der(16)	mat-del(1pter-p13.3); mat-amp(1p13.3-qter)	Alternate + CIN	Yes	Yes	Yes	Yes
		E04	BI112	der(1); der(16)	-	Alternate	Yes	Yes	Yes	Yes
			BI118	der(1); der(16)	-	Alternate	Yes	Yes	Yes	
		E05	BI095	der(1); nor(16)	pat-dup(16pter-p12.1)	Adjacent 1	Yes	No	Yes	Yes
		E06	BI105	der(1); nor(16)	pat-monosomy(1); pat-dup(16pter-p12.1)	Adjacent 1 + CIN	Yes	No	Yes	Yes
		E11	BI091	nor(1); der(16)	mat-trisomy(1); pat-del(16pter-p12.1)	Adjacent 1 + CIN	No	Yes	Yes	Yes
	Paternal t(1;16)(p36.33 ;p12.1) (IVF-cycle 2)	E02	BI337	der(1); der(16)	pat-monosomy(1)	Alternate + CIN	Yes	Yes	Yes	Yes
		E04	BI341	der(1); nor(16)	pat-amp(16pter-p12.1); pat-trisomy(16); pat-del(16q24.1-qter)	Adjacent 1 + CIN	Yes	No	Yes	Yes
		E07	BI312	der(1); nor(16)	pat-dup(16pter-p12.1)	Adjacent 1	Yes	No	Yes	Yes
			BI314	der(1); nor(16)	pat-dup(16pter-p12.1)	Adjacent 1	Yes	No	Yes	Yes
		E10	BI324	--- ; ---	mat-monosomy(1); nullisomy(16)	CIN	No	No	No	Yes

[a] --- means that the blastomere could not be diagnosed for either der(1) or der(16) due to chromosome aneuploidy, i.e. the paternal allele of the chromosome is missing in the cell

Figure S10 | PCR-based validation of siCHILD-based PGD. A, Family PGD016 segregates a mutant dystrophin (*DMD*) gene causing Duchenne Muscular Dystrophy. **B**, Gel electrophoresis images of the PCR products for loci of the *SRY* gene, *DMD* exon 51 and the *FVIII* gene (as a control for presence of X chromosome). **C**, The PCR-products confirmed the accuracy of the method. **D**, Family PGD004 is burdened with a paternal t(1;16)(p36;p12). **E**, Gel electrophoresis images of the PCR products across the breakpoints of the der(1) and der(16) chromosomes, and a control locus of chromosome 16 proximal to the translocation breakpoint. The PCRs were performed on the DNA of the affected sibling (carrier of the der(1) chromosome), the father (balanced carrier of the der(1) and der(16) chromosomes), the mother (containing non-rearranged chromosomes) as well as the single blastomeres used for siCHILD-based PGD. **F**, The PCR-products across the der(1) and der(16) translocation breakpoints confirm the accuracy of siCHILD-based PGD for all single blastomeres.

Figure S11

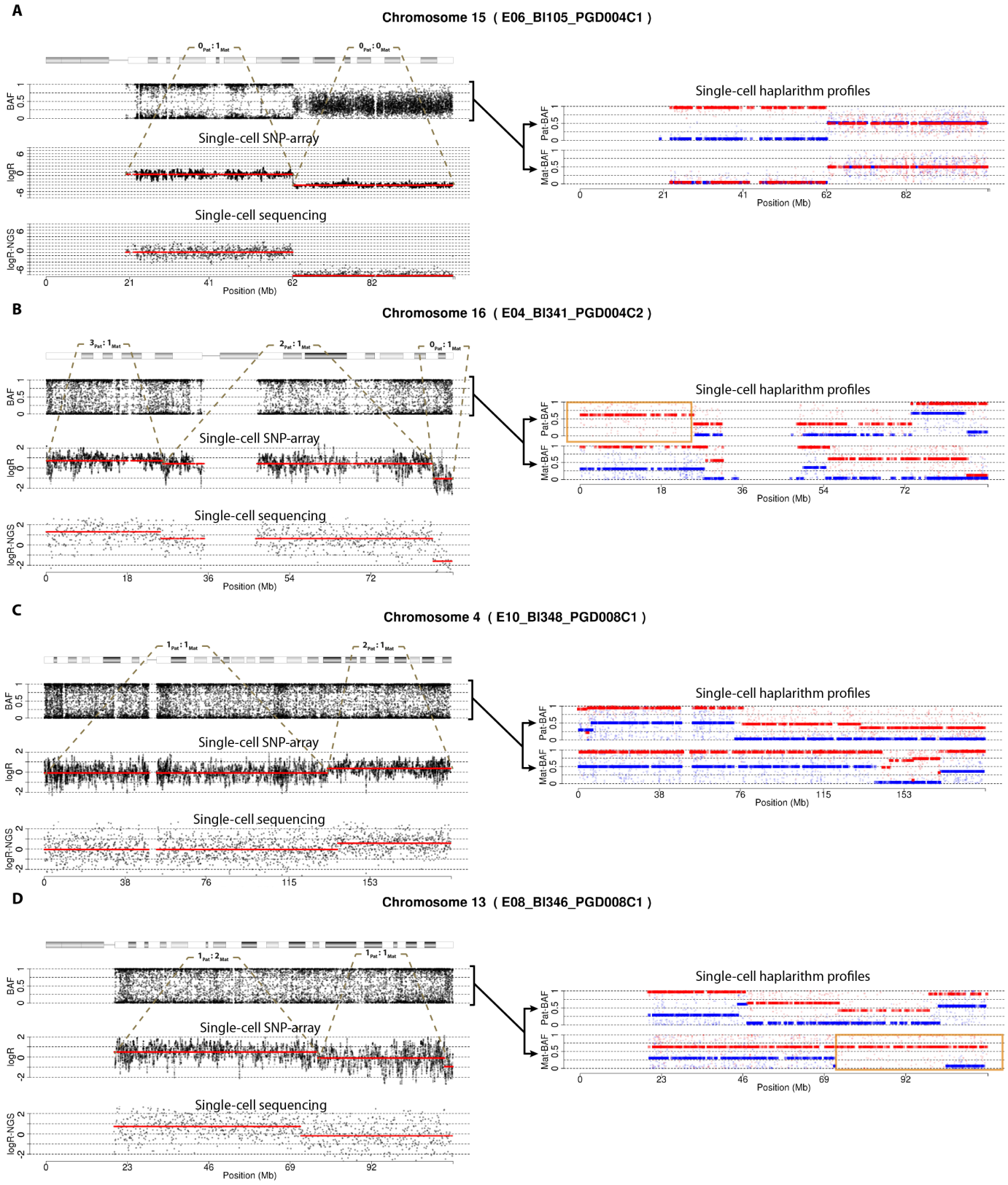

Figure S11 | Single-cell copy number analysis supervised by haplarithmisis: segmental chromosome anomalies. Single-cell copy number profiles determined by both SNP-array and single-cell sequencing analyses are leveraged by haplarithmisis. The allelic ratio of each segment is indicated. **A**, A maternal monosomy 15 with a segmental nullisomy 15. **B**, Chromosome 16 displaying a 16pter paternal amplification, an interstitial paternal duplication and a 16qter deletion on the paternal allele. **C**, A paternal 4qter segmental duplication. **D**, A meiotic trisomy with a copy neutral segment. The orange frame indicates the paternal or maternal profile segment that could not be haplotyped with discrete SNP genotypes, which is due to a duplication of that segment in the individual that served as a seed for phasing of the parental discrete genotypes. In contrast, the reciprocal maternal or paternal single-cell haplarithm, respectively, does reveal the allelic ratio of that segment.

Figure S12

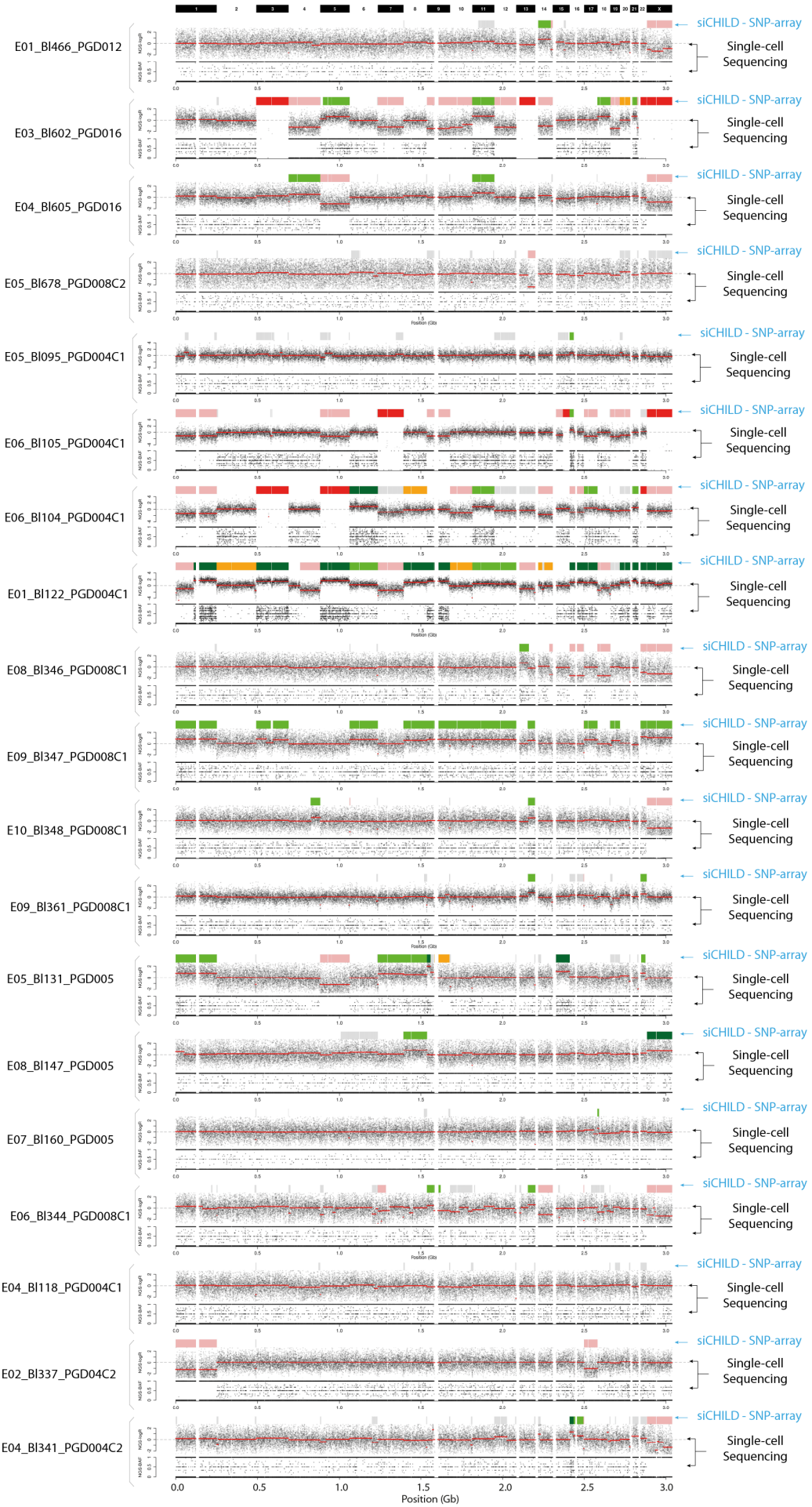
E01_Bl466_PGD012
E03_Bl602_PGD016
E04_Bl605_PGD016
E05_Bl678_PGD008C2
E05_Bl095_PGD004C1
E06_Bl105_PGD004C1
E06_Bl104_PGD004C1
E01_Bl122_PGD004C1
E08_Bl346_PGD008C1
E09_Bl347_PGD008C1
E10_Bl348_PGD008C1
E09_Bl361_PGD008C1
E05_Bl131_PGD005
E08_Bl147_PGD005
E07_Bl160_PGD005
E06_Bl344_PGD008C1
E04_Bl118_PGD004C1
E02_Bl337_PGD04C2
E04_Bl341_PGD004C2
siCHILD - SNP-array
Single-cell Sequencing
0.0
0.5
1.0
1.5
2.0
2.5
3.0
Position (Gb)

Figure S12 | Single-cell sequencing confirms the single-cell copy number landscapes determined by SNP-array analysis. siCHILD-determined copy number profiles of 19 single blastomeres were confirmed by single-cell sequencing. For each single blastomere the first panel is a heatmap of siCHILD-determined copy number profiles corroborated by haplarithm patterns (red for homozygous deletions, pink for hemizygous deletions, light green for a duplication, dark green for an amplification and orange for a uniparental isodisomy). Aberrant logR-segments (> 0.15 or < -0.3) not corroborated by a haplarithm pattern are depicted in grey. For cells analyzed in the framework of translocation PGD cases, DNA-imbalances smaller than 3 Mb corroborated by the haplotype of a derivative chromosome of the parental reciprocal translocation are depicted as well. The second and third panels show the logR- and BAF-values derived form single-cell sequencing data (genomic bins of 100kb in size were applied for focal read-depth analysis).

Figure S13

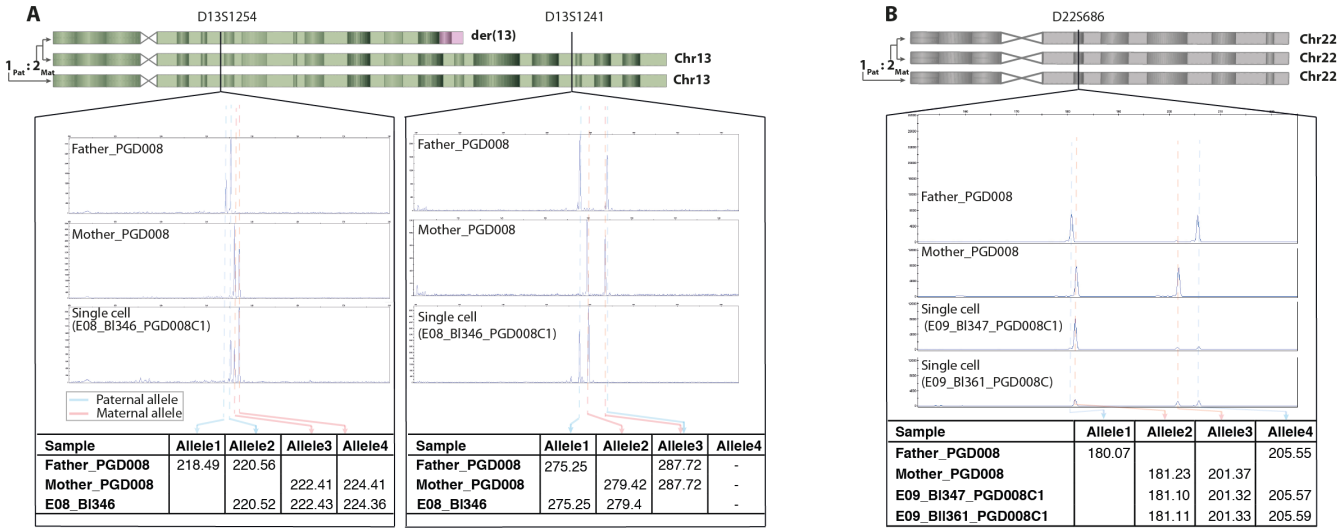

Sample	Allele1	Allele2	Allele3	Allele4
Father_PGD008	218.49	220.56		
Mother_PGD008			222.41	224.41
E08_Bl346		220.52	222.43	224.36

Sample	Allele1	Allele2	Allele3	Allele4
Father_PGD008	275.25		287.72	-
Mother_PGD008		279.42	287.72	-
E08_Bl346	275.25	279.4		-

Sample	Allele1	Allele2	Allele3	Allele4
Father_PGD008	180.07			205.55
Mother_PGD008		181.23	201.37	
E09_Bl347_PGD008C1		181.10	201.32	205.57
E09_Bl361_PGD008C1		181.11	201.33	205.59

Figure S13 | STR-marker analyses. A, STR-length profiles proving a meiotic trisomy for chromosome 13 in cell Bl346 of embryo E08 that was identified via haplarithmisis. This blastomere inherited two maternal chromosomes (a der(13) of t(6;13;16), and a normal chromosome 13) as well as a paternal chromosome 13. The vertical dashed lines indicate the parental alleles, which are present in the table of each STR marker (pink for maternal alleles and blue for paternal alleles). **B**, STR-length profiles proving a meiotic trisomy of chromosome 22 in cells Bl347 and Bl361 of embryo E09 that was identified via haplarithmisis. The father has “allele1” and “allele4”, while the mother carries “allele2” and “allele3”. The two blastomeres contain both alleles of the mother and one “allele4” of the father. Note that these assays have been performed on single-cell MDA products.

Figure S14

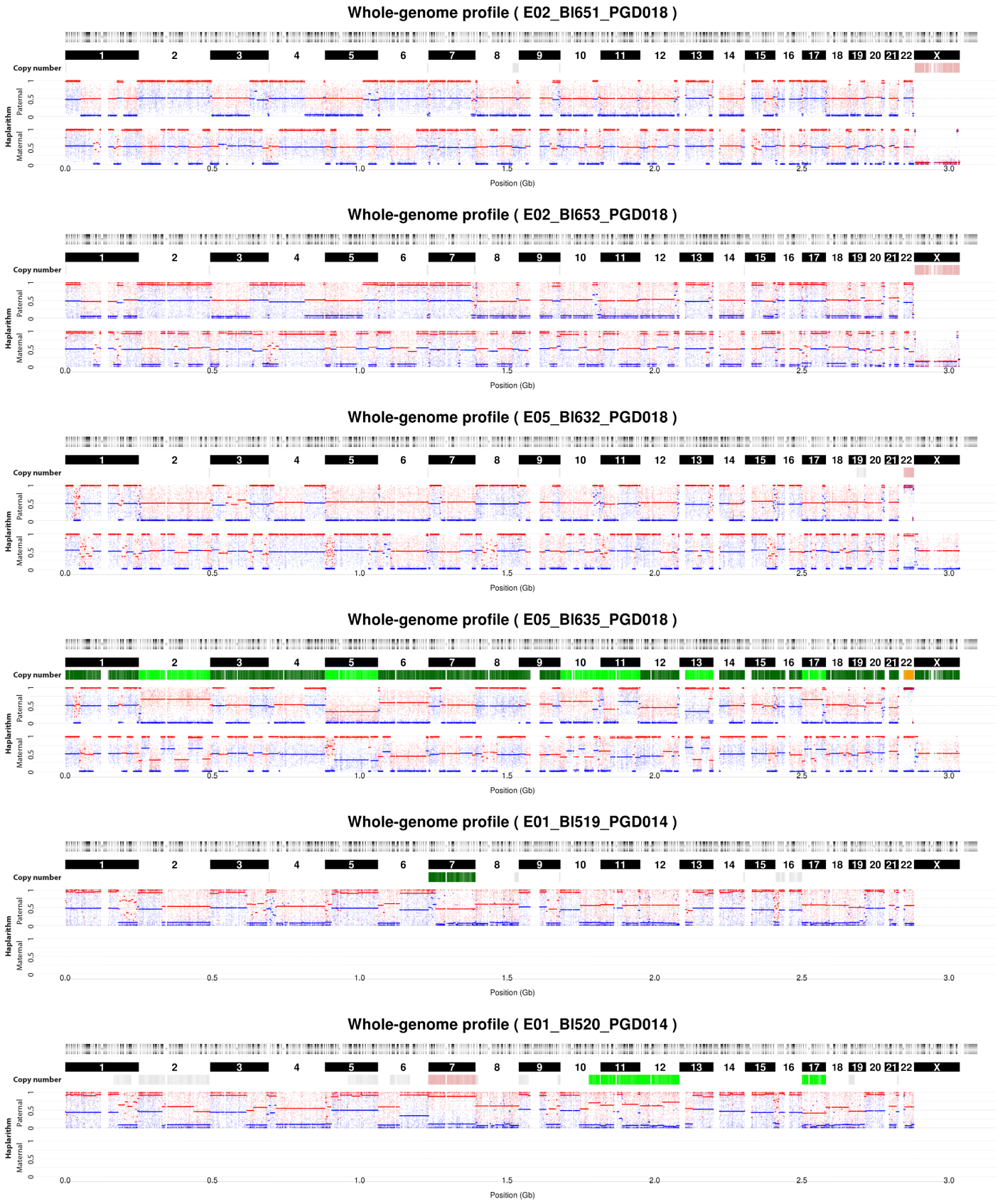
Whole-genome profile (E02_BI651_PGD018)
Whole-genome profile (E02_BI653_PGD018)
Whole-genome profile (E05_BI632_PGD018)
Whole-genome profile (E05_BI635_PGD018)
Whole-genome profile (E01_BI519_PGD014)
Whole-genome profile (E01_BI520_PGD014)
Copy number
Haplarithm
Paternal
Maternal
Position (Gb)

Figure S14 (continued)

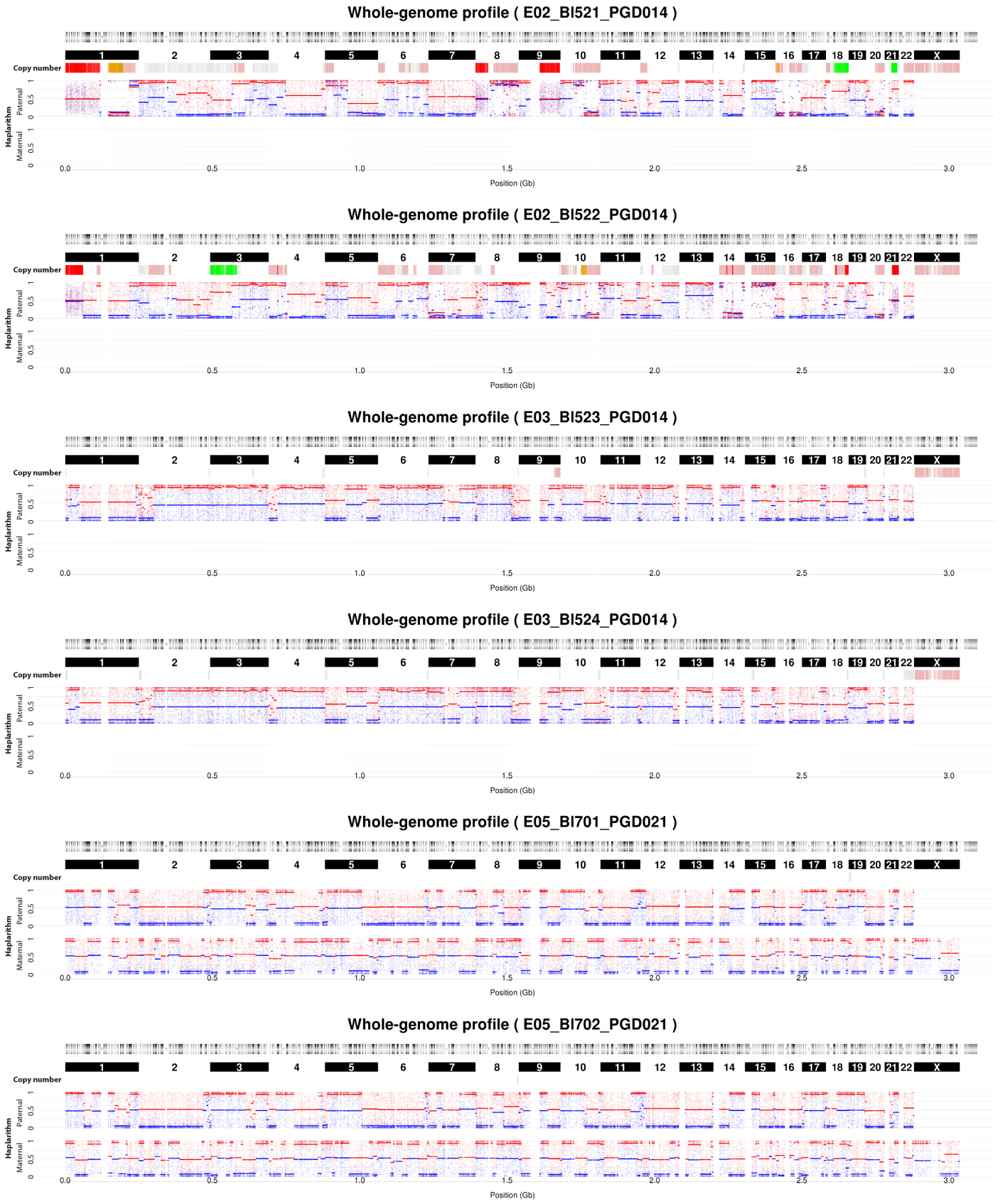

Figure S14 (continued)

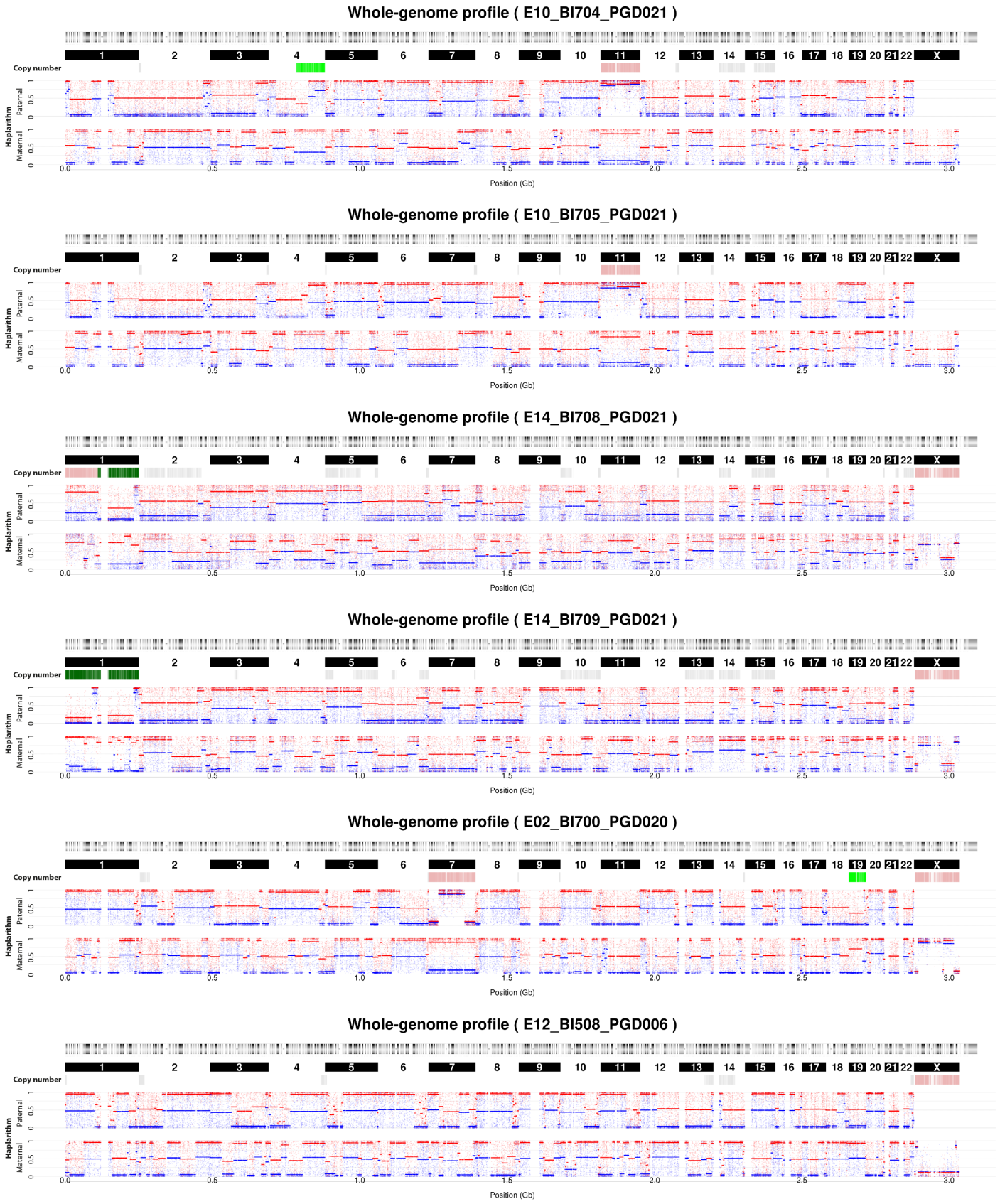

Figure S14 (continued)

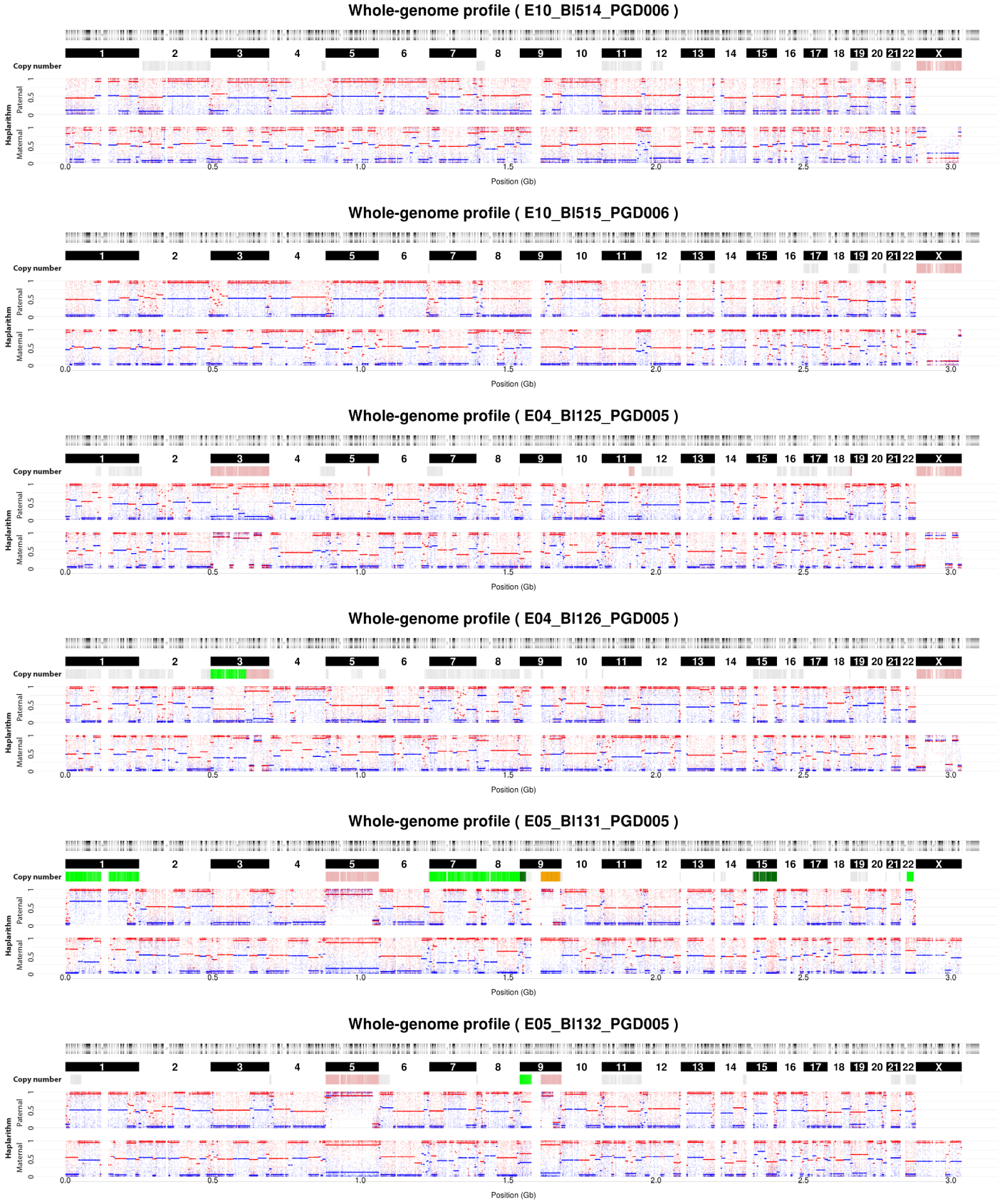

Figure S14 (continued)

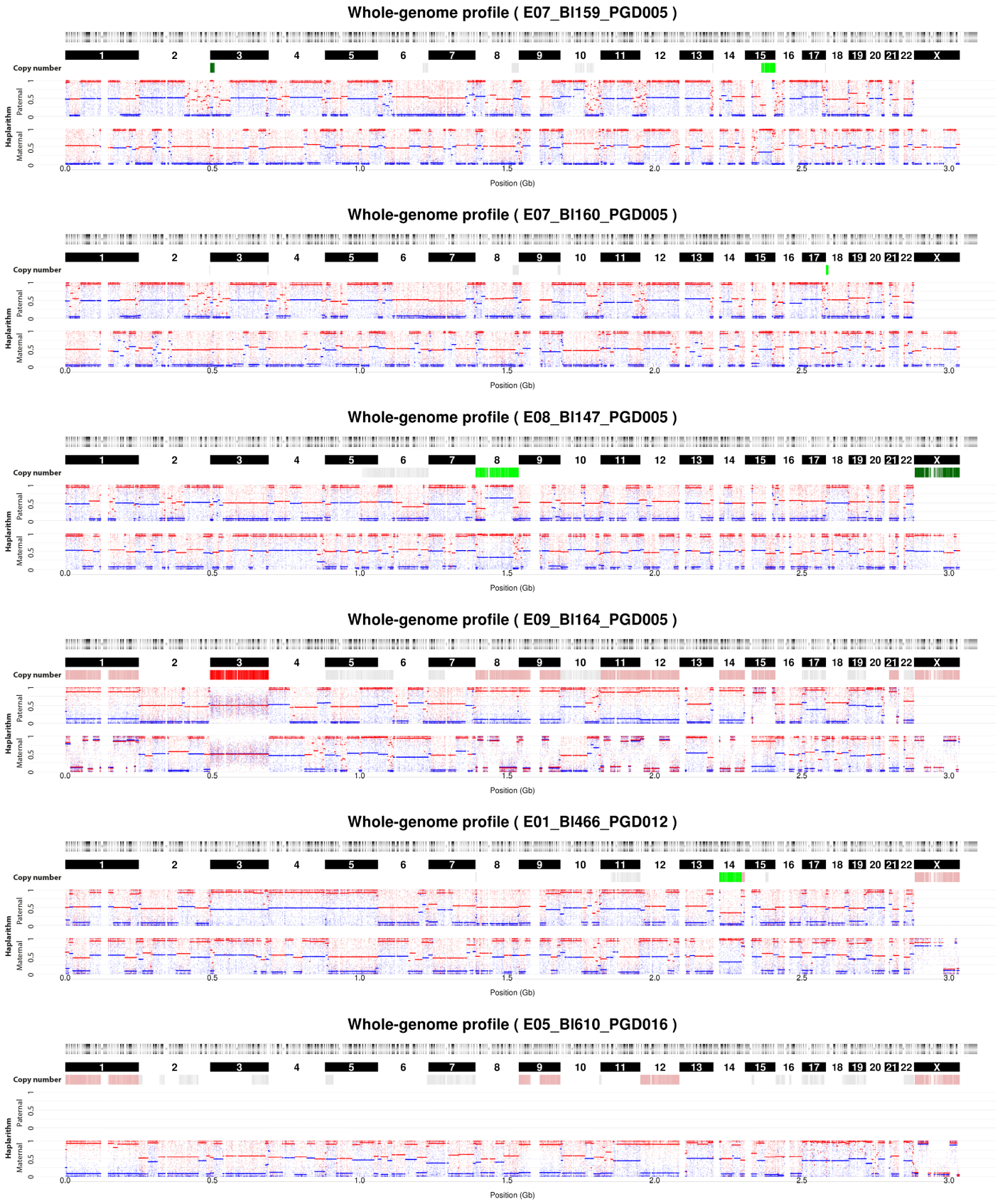

Figure S14 (continued)

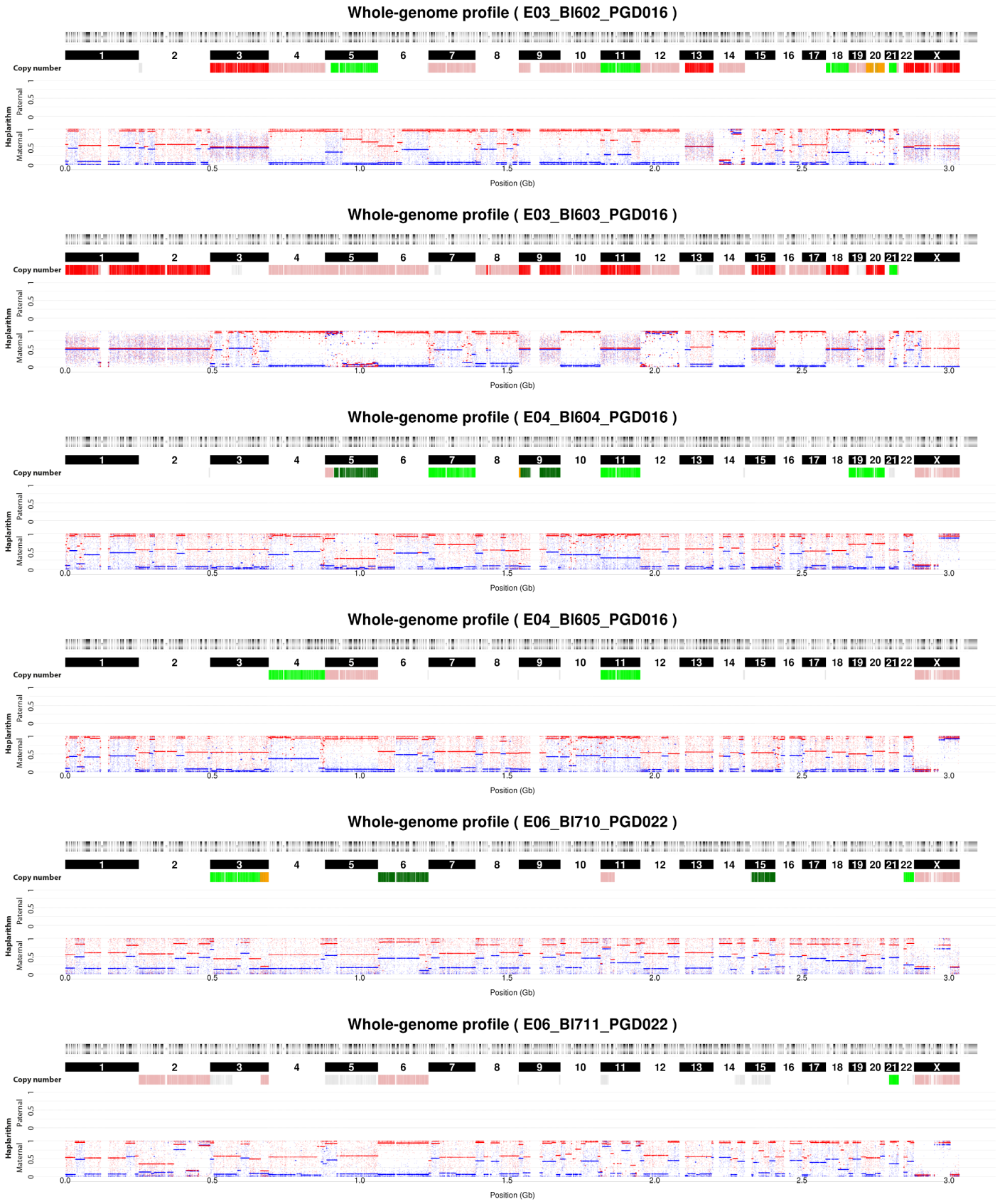

Figure S14 (continued)

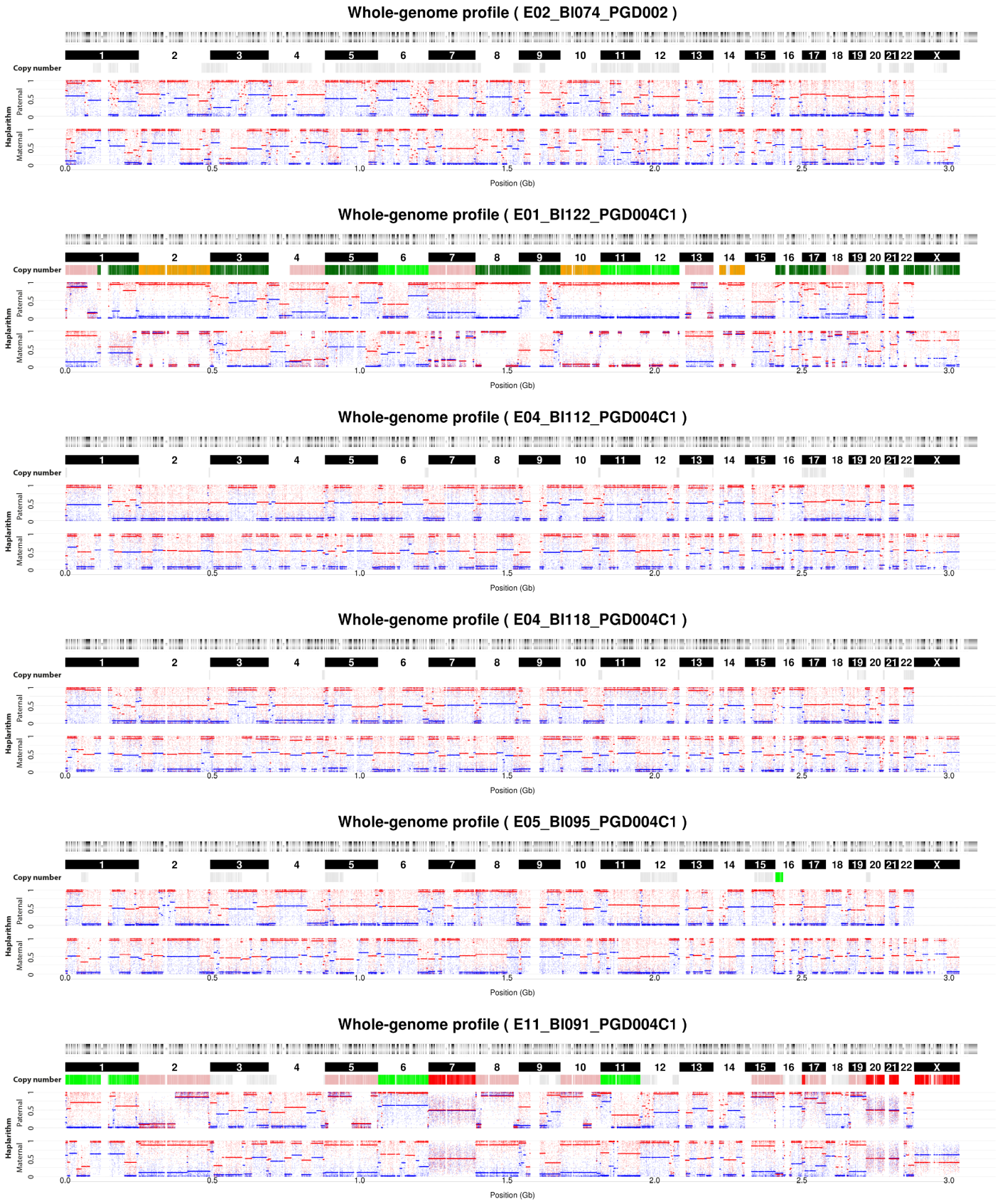

Figure S14 (continued)

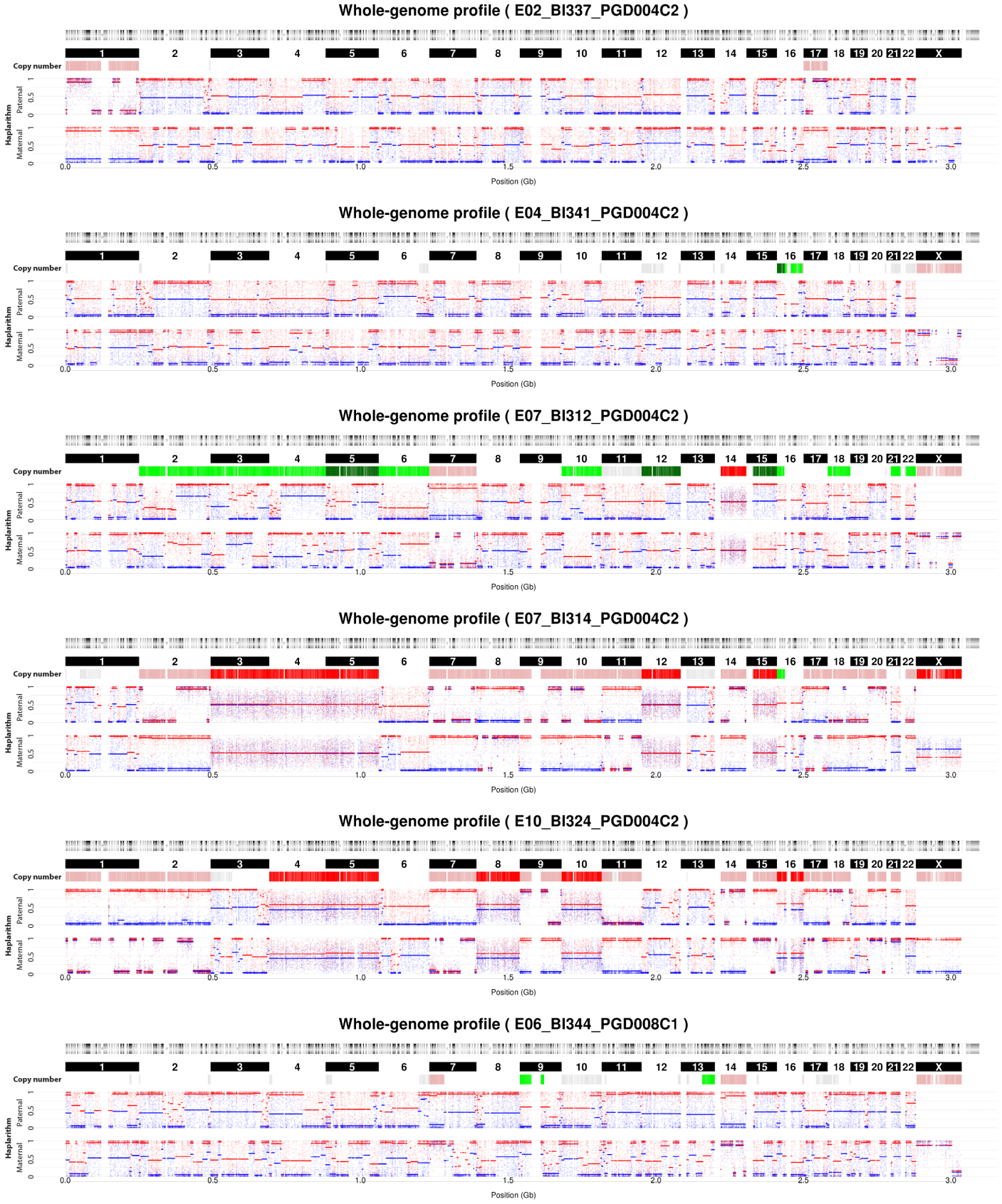

Figure S14 (continued)

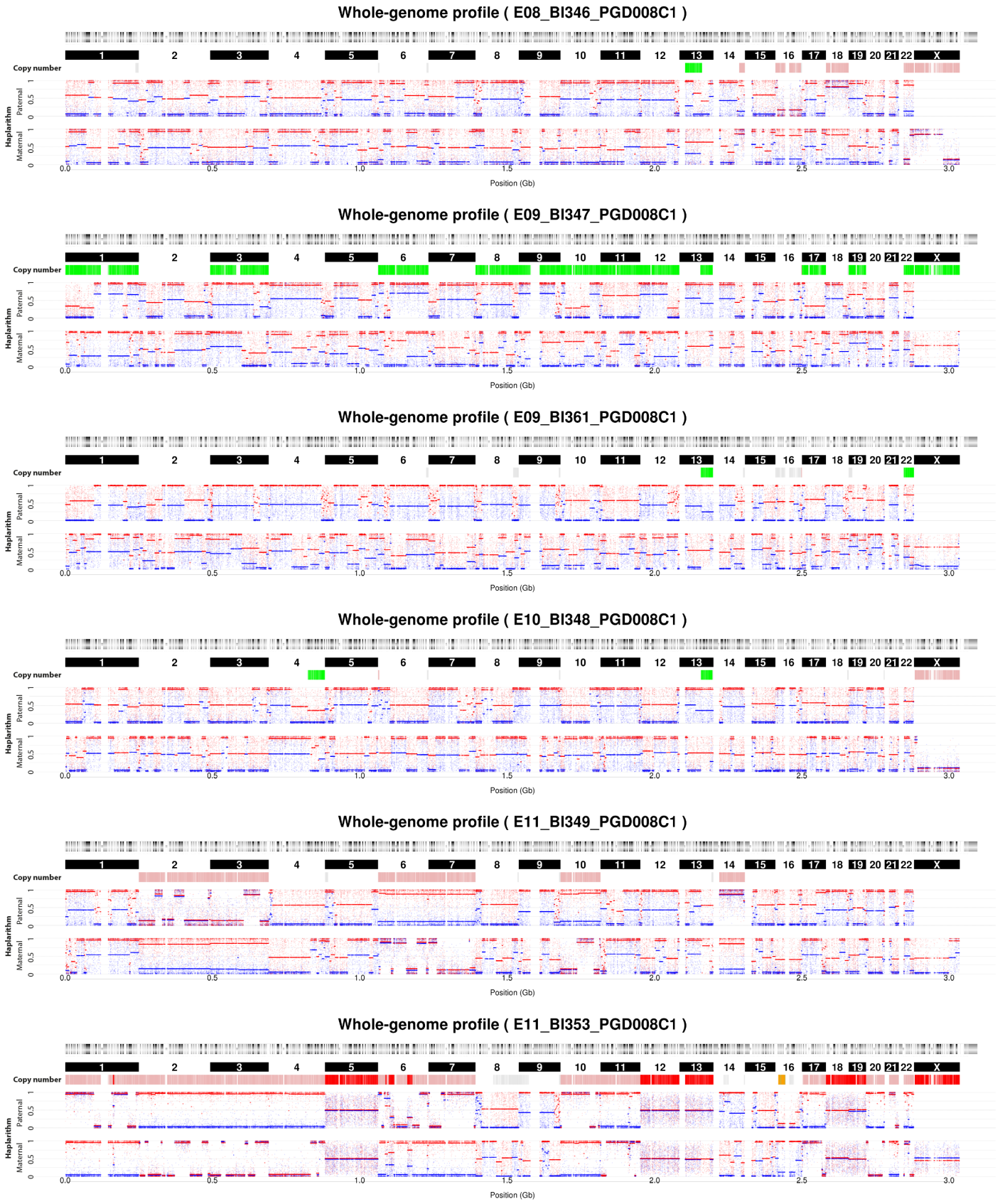

Figure S14 (continued)

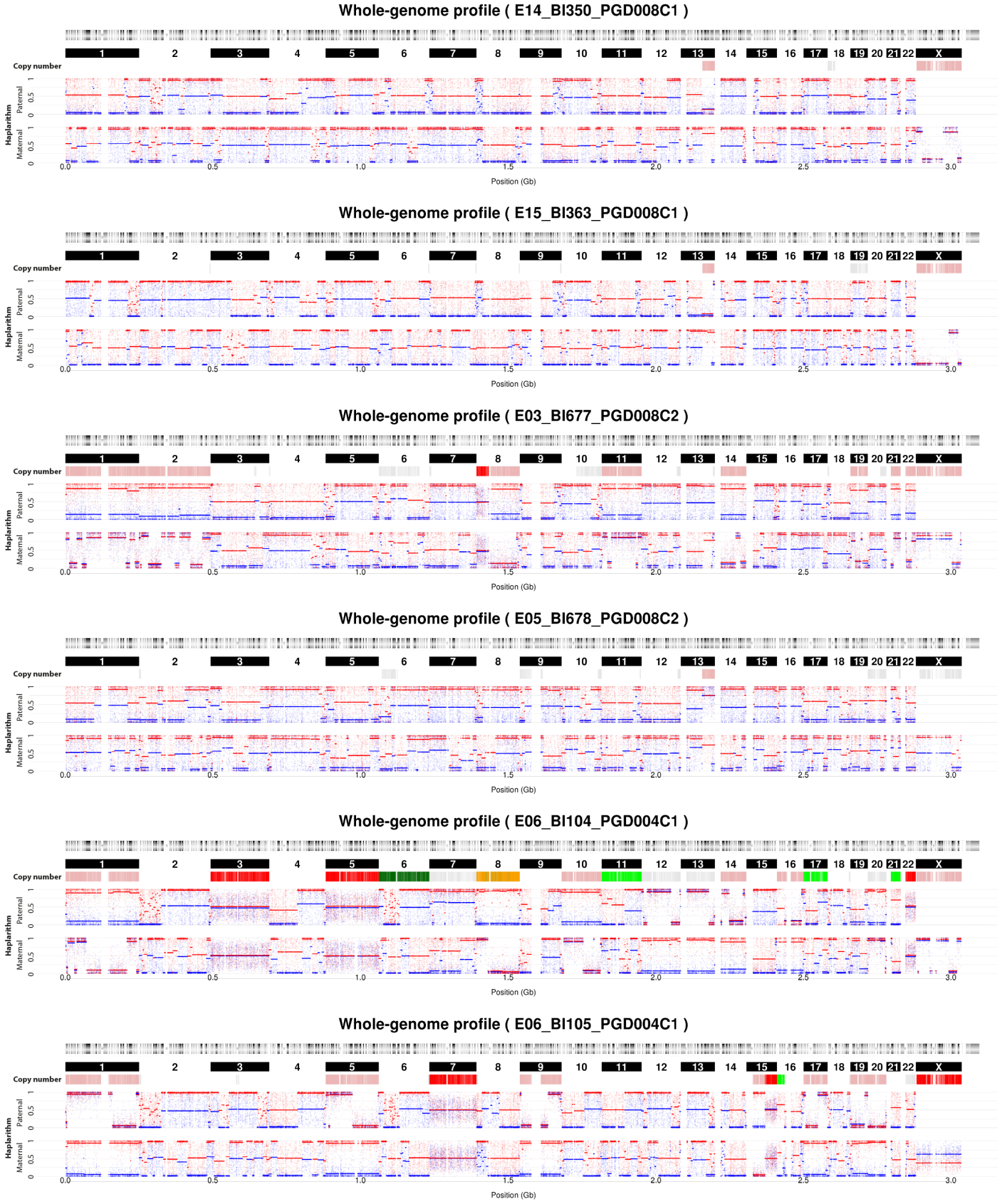

Figure S14 | siCHILD copy number and haplarithm profiles for all 60 single blastomeres. For each single blastomere we show from top to bottom: (i) genome-wide DNA-copy number maps. Aberrant logR-segments (> 0.15 or < -0.3) corroborated by a distinctive haplarithm pattern are depicted. Aberrant logR-segments not corroborated by a haplarithm pattern are depicted in grey. For cells analyzed in the framework of translocation PGD cases, DNA-imbalances smaller than 3 Mb corroborated by the haplotype of a derivative chromosome of the parental reciprocal translocation are depicted as well. (ii) Genome-wide paternal haplaritm and (iii) maternal haplarithm profiles.

Table S1 | QC-by-parents formulas.

QC-by-parents	
ADI =	$\left(\frac{Total\ number\ of\ single-cell\ htz\ SNP-calls\ with\ parental\ SNP-calls\ of\ identical\ homozygosity}{Total\ number\ of\ called\ SNPs\ in\ the\ single\ cell\ that\ have\ parental\ SNP-calls\ of\ identical\ homozygosity}\right)\times 100$
ADO =	$\left(\frac{Total\ number\ of\ single-cell\ hmz\ SNP-calls\ with\ parental\ SNP-calls\ of\ oposite\ homozygosity}{Total\ number\ of\ called\ SNPs\ in\ the\ single\ cell\ that\ have\ parental\ SNP-calls\ of\ oposite\ homozygosity}\right)\times 100$
ADOI =	$\left(\frac{Total\ number\ of\ single-cell\ hmz\ SNP-calls\ oposite\ to\ \ parental\ SNP-calls\ of\ identical\ homozygosity}{Total\ number\ of\ called\ SNPs\ in\ the\ single\ c\ \ ll\ that\ have\ parental\ SNP-calls\ of\ identical\ homozygosity}\right)\times 100$
ADI-sc =	$\left(\frac{Total\ number\ of\ single-cell\ htz\ SNP-calls\ that\ have\ parental\ SNP-calls\ of\ identical\ homozygosity}{Total\ number\ of\ single-cell\ htz\ SNP-calls}\right)\times 100$
ADO-sc =	$\left(\frac{Total\ number\ of\ single-cell\ hmz\ SNP-calls\ that\ have\ parental\ SNP-calls\ of\ oposite\ homozygosity}{Total\ number\ of\ single-cell\ hmz\ SNP-calls}\right)\times 100$
ADOI-sc=	$\left(\frac{Total\ number\ of\ single-cell\ hmz\ SNP-calls\ oposite\ to\ parental\ SNP-calls\ of\ identical\ homozygosity}{Total\ number\ of\ single-cell\ hmz\ SNP-calls}\right)\times 100$

Table S2 | Rules for parent-of-origin value assignment.

Father's SNP-call	Mother's SNP-call	Conceptus' SNP-call	P (paternal parent-of-origin value)	M (maternal parent-of-origin value)
AA	BB	AA	1	0
AA	BB	BB	0	1
AA	AB	BB	0	0.5
AB	AA	BB	0.5	0
AB	BB	AA	0.5	0
BB	AA	BB	1	0
BB	AA	AA	0	1
BB	AB	AA	0	0.5

Table S3 | Retained chromosomes for the final trimmed mean correction of the logR-values. The chromosomes retained for trimmed mean corrections of each single blastomere are indicated with green rectangles.

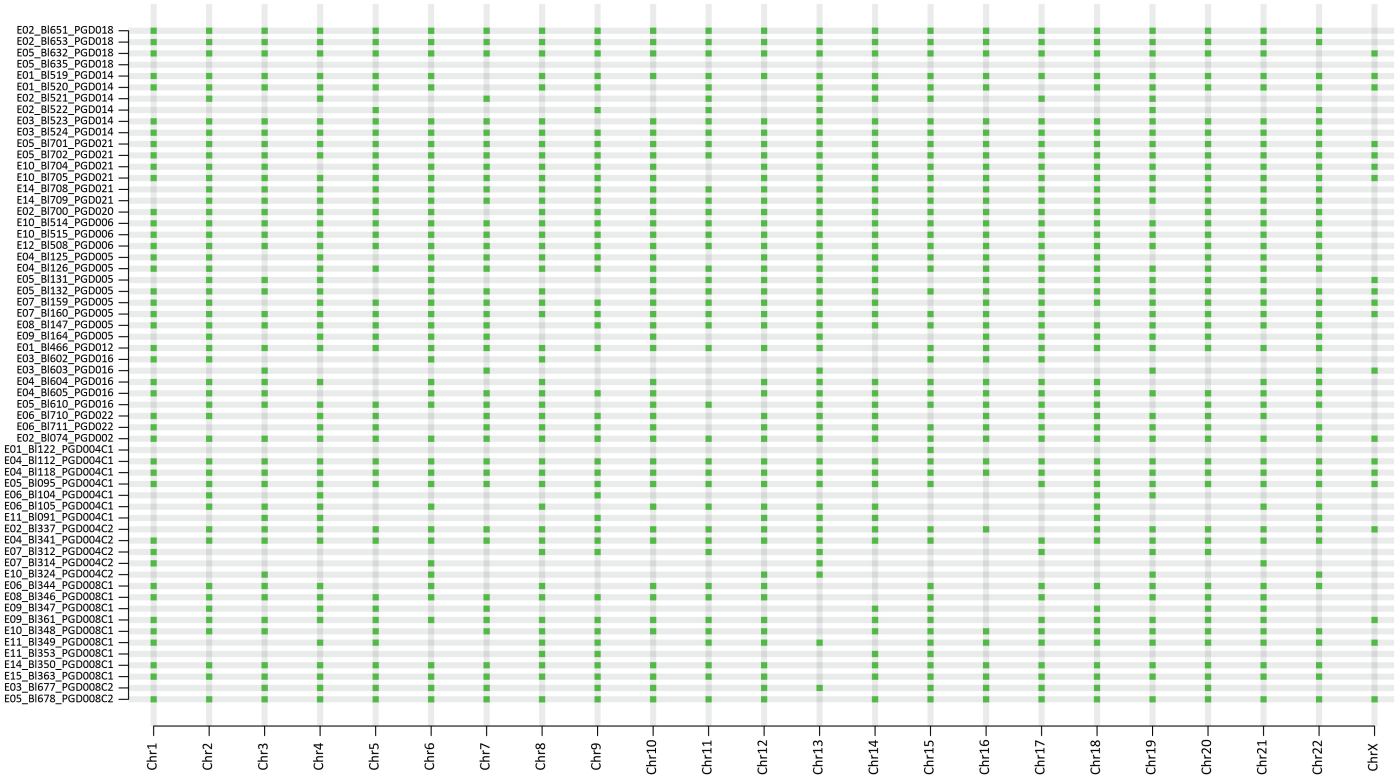

Table S4 | A detailed overview of the embryos involved in this study.

Family	Condition	origin	ART data					Embryo quality data (d3)				Traditional PGD data		
			ART method	mature oocytes	fertilized	biopsied	transfered/ frozen	Embryo	# of cells	Fragmen-tation	Asymmetry	Cells biopsied	PGD Method	Probes for FISH/ STR markers for PCR
PGD002	t(10;16)(q23;p13.3)	mat	IVF	7	7	6	1/0	E02	6	2	2	2	FISH	TelVysion 10q (D10S2290,ABBOTT), TelVysion 16p (16pTEL05,ABBOTT); CEP 10 (10p11.1-q11.1,ABBOTT)
								E03	7	0	1			
PGD004C1	t(1;16)(p36;p12)	pat	ICSI	12	8	6	1/0	E01	3	2	1	2	FISH	TelVysion 16p (16pTEL05,ABBOTT); CEP 16 (D16Z3,ABBOTT); CEP 1 (D1Z5,ABBOTT)
								E04	4	1	1			
								E05	7	2	1			
								E06	7	2	1			
								E09	6	3	1			
								E11	8	2	1			
PGD004C2				13	11	7	0	E02	4	1	1			
								E04	5	3	1			
								E06	8	3	1			
								E07	6	4	1			
								E10	7	1	1			
PGD005	Xpdel	mat	IVF	9	9	5	1/1	E04	4	1	1	2	FISH	RP11-323F16 (X:7446551-7622830, 32K clone set, CHORI); CEP X (DXZ1, ABBOTT); CEP Y (DYZ1, ABBOTT)
								E05	5	1	2			
								E06	6	0	0			
								E07	8	2	1			
								E08	5	1	2			
								E09	5	4	1			
PGD006C1	17qdel	pat	IVF	6	5	4	1/0	E04	6	2	2	2	FISH	CEP17 (D17Z1,ABBOTT); RP11-293K20 (17: 67077180-67260438, 32K clone set, CHORI) (deletion specific); RP11-283E7(17: 66771289-66941661, 32K clone set, CHORI) (flanking the deletion)
PGD006C2				14	14	9	2/2	E07	6	0	0			
								E10	8	0	0			
								E12	8	0	0			
								E13	5	1	0			
PGD008C1	t(6;13;16)	mat	ICSI	15	14	9	0	E02	4	4	1	1	FISH	TelVysion 6p (6pTEL48,ABBOTT); TelVysion 16q (16qTEL013,ABBOTT); CEP 6 (D6Z1,ABBOTT)
								E04	8	2	1			
								E06	7	3	2			
								E08	6	3	2			

								E09	8	2	2			
								E10	8	3	2			
								E11	8	2	1			
								E14	9	1	1			
								E15	7	2	2			
PGD008C2				8	7	6	1/0	E03	6	1	2			
								E05	8	1	1			
								E06	7	1	1			
								E07	8	2	1			
								E08	7	2	1			
PGD012	X-linked Hemophilia A	mat	IVF	3	3	3	1/0	E01	6	1	2	1	FISH	CEP X/ CEP Y (DXZ1/ DYZ3, ABBOTT); CEP Y (DYZ1, ABBOTT)
								E03	7	2	1			
PGD014	autosomal dominant CMT1a	pat	ICSI	4	4	4	0/0	E01	8	1	0	2	PCR	D17S2220, D17S2227, D11S1220TN, D17S2230, D17S2229, PMP22str23AC
								E02	8	1	1			
								E03	12	1	0			
PGD016	X-linked DMD	mat	IVF	5	5	4	1	E02	2	1	1	2	FISH	G248P89342F12 (X:31676064-31717812,fosmid, CHORI) (deletion specific); G248P84179B5 (X:31798627-31839362 ,fosmid, CHORI) (deletion specific); RP11-724L13 (X: 31244652-31393058, 32K clone set, CHORI) (flanking the deletion); CEP Y (DYZ1, ABBOTT)
								E03	11	0	1			
								E04	8	1	1			
								E05	13	1	1			
PGD018	autosomal recessive HbS/HbC	mat/ pat	ICSI	10	9	9	1/4	E02	10	3	0	2	PCR	D11S1760, D11S2351
								E05	6	3	1			
PGD020	autosomal recessive CF	mat/ pat	ICSI	10	8	6	1/4	E02	8	1	1	1	PCR	D7S677, IVS17BTA, IVS8CA, D7S633, CFTRSTR15CA, dF508, CFTRSTR30AC
PGD021	autosomal recessive CF	mat/ pat	ICSI	19	11	10	1/1	E05	8	2	0	1	PCR	D7S677, IVS17BTA, IVS8CA, D7S633, CFTRSTR15CA, dF508, CFTRSTR30AC
								E10	8	0	0			
								E14	8	1	0			
PGD021	autosomal dominant DBA1	pat	ICSI	19	11	10	1/1	E05	8	2	0	1	PCR	RPS19GTB, D19S197, D19S198, RPS19AG19, D19S423
								E10	8	0	0			
								E14	8	1	0			
PGD022	X-linked FRAXA	mat	ICSI	13	9	9	2/0	E06	8	0	1	1	PCR	AMEL, DXS6687, DXS548, FMR1STR22CA, DXS998

Table S5 | General single-cell sequencing information.

Sample	# Sequenced reads ($x10^6$)	# Mapped reads ($x10^6$)	Mapped reads (%)	Read length	Depth of coverage
E05_Bl131_PGD005	18.2	17.1	94.5	101	0.56
E08_Bl147_PGD005	16.2	15.4	95.5	101	0.50
E07_Bl160_PGD005	9.6	9.1	94.8	101	0.30
E06_Bl344_PGD008C1	15.3	14.6	95.6	101	0.48
E08_Bl346_PGD008C1	15.6	14.9	95.9	101	0.49
E09_Bl347_PGD008C1	22.6	21.6	95.3	101	0.70
E10_Bl348_PGD008C1	21.1	20.2	95.7	101	0.66
E09_Bl361_PGD008C1	15.3	14.6	95.3	101	0.48
E01_Bl466_PGD012	13.0	12.4	95.8	101	0.41
E03_Bl602_PGD016	15.1	14.3	94.7	101	0.47
E04_Bl605_PGD016	20.2	19.1	94.4	101	0.62
E05_Bl678_PGD008C2	16.9	16.2	95.7	101	0.53
E04_Bl118_PGD004C1	20.7	19.7	94.8	101	0.64
E02_Bl337_PGD004C2	21.1	20.0	94.9	101	0.65
E04_Bl341_PGD004C2	14.6	13.9	94.9	101	0.45
E05_Bl095_PGD004C1	15.3	14.3	93.3	101	0.47
E06_Bl104_PGD004C1	27.8	26.1	94.1	101	0.85
E06_Bl105_PGD004C1	24.8	23.4	94.4	101	0.76
E01_Bl122_PGD004C1	35.6	33.3	93.6	101	1.09

Table S6 | 1D-MF reproducibility for pairs of diploid blastomeres derived from the same embryo.

Family	Embryo	Blastomere 1	Blastomere 2	Paternal (%)	Maternal (%)
PGD018	E02	Bl651	Bl653	99.55	99.30
PGD021	E05	Bl701	Bl702	99.66	99.16
PGD004C1	E04	Bl112	Bl118	99.31	98.95
PGD006	E10	Bl514	Bl515	98.51	97.91

Table S7 | PGD for autosomal recessive or dominant Mendelian disorders

Family	Condition	Embryo	Diagnosis				
			Blastomere	siCHILD-based PGD [b]	Blastomere	PCR-based PGD	Concordant
PGD018	Chr11p15.4 *HBB* gene Sickle-cell disease Autosomal recessive	E02	Bl651	Affected - HbC/HbS	Sister-Bl1	Affected - HbC/HbS	Yes
			Bl653	Affected - HbC/HbS	Sister-Bl2	Affected - HbC/HbS	
		E05	Bl632	Affected - HbS/HbS	Sister-Bl1	Affected- HbS/HbS	Yes
			Bl635	Affected - HbS/HbS [c]	Sister-Bl2	Affected- HbS/HbS	
PGD014	17p12 *PMP22* gene – paternal mutation Charcot-Marie Tooth Autosomal dominant	E01	Bl519	Affected	Sister-Bl1	Affected	Yes
			Bl520	Affected, including a mitotic trisomy 17 with two paternal affected alleles and one maternal normal allele present	Sister-Bl2	Affected	
		E02	Bl521	Affected	Sister-Bl1	Affected-mosaic	Yes
			Bl522	Affected locus is present, but a structural rearrangement affects chromosome 17	Sister-Bl2	Inconclusive	
		E03	Bl523	Affected	Sister-Bl1	Affected	Yes
			Bl524	Affected	Sister-Bl2	Affected	
PGD021 [a]	7q31.2 *CFTR* gene Cystic Fibrosis Autosomal recessive	E05	Bl701	Maternal mutation carrier	Sister-Bl1	Maternal mutation carrier	Yes
			Bl702	Maternal mutation carrier			
		E10	Bl704	Non-carrier	Sister-Bl1	Non-carrier	Yes
			Bl705	Non-carrier [d]			
		E014	Bl708	Affected	Sister-Bl1	Affected	Yes
			Bl709	Affected			
	19q13.2 *RPS19* gene – paternal mutation Diamond-Blackfan anemia Autosomal dominant	E05	Bl701	Affected	Sister-Bl1	Affected	Yes
			Bl702	Affected			
		E10	Bl704	Affected	Sister-Bl1	Affected	Yes
			Bl705	Affected			
		E014	Bl708	Non-carrier	Sister-Bl1	Non-carrier	Yes
			Bl709	Non-carrier			
PGD020	7q31.2 *CFTR* gene Cystic Fibrosis Autosomal recessive	E02	Bl700	normal allele, but paternal monosomy 7	Sister-Bl1	normal allele, but paternal monosomy 7q31.2	Yes
Family	**Condition**	**Embryo**	**Blastomere**	**siCHILD-based PGD**	**Blastomere**	**FISH-based PGD**	**Concordant**
PGD006	Paternal del(17q) Autosomal dominant	E10	Bl514	Non-carrier	Sister-Bl1	nor(17q)	Yes
			Bl515	Non-carrier	Sister-Bl2	nor(17q)	
		E12	Bl508	Affected	Sister-Bl1	del(17q)	Yes

[a] This family was screened for both autosomal recessive and autosomal dominant monogenic disorders by siCHILD. Since paternal grandparental DNA and DNA of a sibling were available, both phasing strategies were applied.

[b] For detailed DNA copy number interpretation across the region of interest and genome wide, see figure 7 and the section on aneuploidy screening of the main text.

[c] Blastomere 635 was interpreted as a tetraploid cell (see also **Fig. 7**). For chromosome 11, which carries the HBB-locus, one copy is lost, resulting in two paternal and one maternal alleles remaining, all carrying the HbS mutated allele. [d] The disease locus is located ≥98 SNPs (max 170 SNPs) from a putative homologous recombination site.

Table S8 | PGD for X-linked recessive Mendelian disorders

Family	X-linked recessive disorder	Embryo	Diagnosis				
			Blastomere	siCHILD-based PGD [a]	Blastomere	FISH-based PGD	Concordant
PGD005	del(Xp22.31) syndrome	E04	Bl125	Affected male – del(Xp22.31)	-	-	-
			Bl126	Affected male – del(Xp22.31)			
		E05	Bl131	Non-carrier female	-	-	-
			Bl132	Non-carrier female			
		E07	Bl159	Carrier female – del(Xp22.31)	-	-	-
			Bl160	Carrier female – del(Xp22.31)			
		E08	Bl147	Non-carrier female [b]	-	-	-
		E09	Bl164	Non-carrier male	-	-	-
PGD012	Xq28 *Factor VIII* gene Hemophilia A	E01	Bl466	Affected male [c]	Sister-Bl1	male	Yes
PGD016	Xp21.2-21.1 *DMD* gene Duchenne Muscular Dystrophy	E03	Bl602	--- [d]	Sister-Bl1	Non-carrier; monosomy X	Yes [e]
			Bl603	Non-carrier female	Sister-Bl2	Inconclusive	
		E04	Bl604	Non-carrier male	Sister-Bl1	Non-carrier male	Yes
			Bl605	Non-carrier male	Sister-Bl2	Non-carrier male [f]	
		E05	Bl610	Carrier male	Sister-Bl1	Carrier female	No [g]
		Embryo	**Blastomere**	**siCHILD-based PGD**	**Blastomere**	**PCR-based PGD**	**Concordant**
PGD022	Xq27.3-q28 *FMR1* gene Fragile X syndrome	E06	Bl710	Non-carrier male	Sister-Bl1	Non-carrier male	Yes
			Bl711	Non-carrier male			

[a] For detailed DNA copy number interpretation across the region of interest and genome wide, see figure 7 and the section on aneuploidy screening of the main text.

[b] This cell was in addition interpreted to contain a DNA-gain for the X-chromosome.

[c] The allelic origin of the FVIII gene, which is located at the tip of the long arm of chromosome X, was scored based on the most Xq-terminal haplotype block.

[d] siCHILD detected a nullisomy X in blastomere Bl602 (see also **Fig. 7**)

[e] FISH-diagnosis can be in agreement with siCHILD-diagnosis, but chromosome mosaicism in the cleavage stage embryo is evident.

[f] One of the two FISHed cells from embryo E04 showed one signal for the X chromosome and two signals for the Y chromosome.

[g] Sex and carrier-ship were independently confirmed by PCR assays on the same single-cell WGA product of blastomere 610, demonstrating that siCHILD-based diagnosis was correct (**Fig. S10**).

Table S9 | PGD for reciprocal translocations

Family	Translocation	Embryo	DIagnosis							
			Blastomere	siCHILD-based PGD			PCRs specific for the derivative chromosomes [c]	Blastomere	FISH-based PGD [d]	Concordant
				Haplotype [a]	Copy number aberration [b]	Segregation				
PGD002	Maternal t(10;16)(q23.2;p13.3)	E02	Bl074	nor(10); nor(16)	-	Alternate	-	Sister-Bl1	nor(10q); nor(cep10); nor(16p)	Yes
								Sister-Bl2	nor(10q); nor(cep10); nor(16p)	
PGD004	Paternal t(1;16)(p36.33;p12.1) (IVF-cycle 1)	E01	Bl122	der(1); der(16)	mat-del(1pter-p13.3); mat-amp(1p13.3-qter)	Alternate + CIN	der(1) pos; der(16) pos	-	-	-
		E04	Bl112	der(1); der(16)	-	Alternate	der(1) pos; der(16) pos	-	-	-
			Bl118	der(1); der(16)	-	Alternate	der(1) pos; der(16) pos			
		E05	Bl095	der(1); nor(16)	pat-dup(16pter-p12.1)	Adjacent 1	der(1) pos; der(16) neg	Sister-Bl1	del(cep1); dup(16p); nor(cep16)	Yes [e]
		E06	Bl105	der(1); nor(16)	pat-monosomy(1); pat-dup(16pter-p12.1)	Adjacent 1 + CIN	der(1) pos; der(16) neg	Sister-Bl1	del(cep1); nor(16p); del(cep16)	Yes [e]
			Bl104	--- ; nor(16)	mat-monosomy(1); pat-monosomy(16)	CIN	-	Sister-Bl2	Inconclusive	
		E11	Bl091	nor(1); der(16)	mat-trisomy(1); pat-del(16pter-p12.1)	Adjacent 1 + CIN	der(1) neg; der(16) pos	Sister-Bl1	del(cep1); del(16p); nor(cep16)	Yes [e]
	Paternal t(1;16)(p36.33;p12.1) (IVF-cycle 2)	E02	Bl337	der(1); der(16)	pat-monosomy(1)	Alternate + CIN	der(1) pos; der(16) pos	-	-	-
		E04	Bl341	der(1); nor(16)	pat-amp(16pter-p12.1); pat-trisomy(16); pat-del(16q24.1-qter)	Adjacent 1 + CIN	der(1) pos; der(16) neg	-	-	-
		E07	Bl312	der(1); nor(16)	pat-dup(16pter-p12.1)	Adjacent 1	der(1) pos; der(16) neg	Sister-Bl1	del(cep1); dup(16p); del(cep16)	Yes [e]
			Bl314	der(1); nor(16)	pat-dup(16pter-p12.1)	Adjacent 1	der(1) pos; der(16) neg	Sister-Bl2	Inconclusive	
		E10	Bl324	--- ; ---	mat-monosomy(1); nullisomy(16)	CIN	der(1) neg; der(16) neg	Sister-Bl1	nor(cep1); dup(16p); dup(cep16)	Yes [e]
								Sister-Bl2	Inconclusive	

[a] --- means that the blastomere could not be diagnosed for either der(1) or der(16) due to chromosome aneuploidy, i.e. the paternal allele of the chromosome is missing in the cell

[b] For detailed DNA copy number interpretation across the region of interest and genome wide, see figure 7 and the section on aneuploidy screening of the main text. Furthermore, 'pat-dup' means a duplication of the paternal allele; 'pat-del' means a deletion of the paternal allele (i.e. maternal allele remains in the cell); 'pat-monosomy' means that the paternal chromosome is retained in the cell (the maternal chromosome is missing); 'pat-trisomy' means that an extra paternal chromosome is present in the cell; 'pat-amp' indicates an amplification of the paternal allele; similar terminology is applied for the maternal allele 'mat-'.

[c] For PGD004 siCHILD imputation results were further confirmed by PCRs specific for der(1) and der(16) on the same single-cell WGA product (**Fig. S10**). 'pos' denotes a positive PCR product; 'neg' a negative PCR.

[d] 'del' means 1 FISH-signal; 'nor' means 2 FISH-signals; 'dup' means 3 FISH-signals

[e] FISH-diagnosis is concordant with siCHILD-diagnosis, but chromosome mosaicism in the cleavage stage embryo is evident.

Table S10 | PGD for a complex chromosome rearrangement (CCR) – maternal t(6;13;16)(p25.1;q21.33;q24.2)

Family	Embryo	Diagnosis					
		Blastomere	siCHILD-based PGD		Blastomere	FISH-based PGD [c]	Concordant
			Haplotype [a]	Copy number aberration [b]			
PGD008 cycle1	E06	Bl344	nor(6); nor(13); der(16)	mat-dup(13q21.33-qter); del(16q24.2-qter)	Sister-Bl1	nor(6p); nor(cep6); del(16q)	Yes
	E08	Bl346	der(6); nor(13)+der(13) ; ---	mat-trisomy(13) (meiosis I error); neu(13q21.33-qter); pat-monosomy(16); neu(16q24.2-qter)	Sister-Bl1	nor(6p); nor(cep6); del(16q)	Yes [d]
	E09	Bl347	nor(6); nor(13); der(16)	pat-trisomy(6); mat-dup(13q21.33-qter); del(16q24.2-qter)	Sister-Bl1	nor(6p); nor(cep6); del(16q)	Yes [d]
		Bl361	nor(6); nor(13); der(16)	mat-dup(13q21.33-qter); del(16q24.2-qter)			
	E10	Bl348	der(6); nor(13); der(16)	mat-del(6pter-p25.1); mat-dup(13q21.33-qter)	Sister-Bl1	Inconclusive	-
	E11	Bl349	der(6); der(13); der(16)	mat-monosomy(6)	Sister-Bl1	Inconclusive	-
		Bl353	--- ; --- ; ---	pat-monosomy(6) with structural rearrangement; nullisomy(13); pat-segmentalUPD(16)			
	E14	Bl350	nor(6); der(13); nor(16)	mat-del(13q21.33-qter)	Sister-Bl1	dup(6p); nor(cep6); nor(16q)	Yes
	E15	Bl363	nor(6); der(13); nor(16)	mat-del(13q21.33-qter)	Sister-Bl1	dup(6p); nor(cep6); nor(16q)	Yes
cycle2	E03	Bl677	nor(6); ### ; ###	-	Sister-Bl1	null(6p); null(cep6); del(16q)	-
	E05	Bl678	der(6); der(13); nor(16)	mat-del(13q21.33-qter)	Sister-Bl1	nor(6p); nor(cep6); dup(16q)	Yes

[a] --- means that the blastomere could not be diagnosed for either der(6), der(13) or der(16) due to chromosome aneuploidy, i.e. the maternal allele of the chromosome is missing in the cell; while ### means that the blastomere could not be diagnosed for either der(6), der(13) or der(16) due to a limited distance of the translocation breakpoint to a homologous recombination-site. The latter was the case in Bl677 of E03: the chromosome 13 breakpoint was located 15 SNPs from a homologous recombination and the breakpoint on chromosome 16 was 43 SNPs away from a homologous recombination.

[b] For detailed DNA copy number interpretation across the region of interest and genome wide, see figure 7 and the section on aneuploidy screening of the main text. Furthermore, 'mat-dup' means a duplication of the maternal allele; 'mat-del' means a deletion affecting the maternal allele (i.e. paternal allele remains in the cell); 'neu' means copy number neutral; 'mat-monosomy' means that the maternal chromosome is retained in the cell (the paternal chromosome is missing); 'mat-trisomy' means that an extra maternal chromosome is present in the cell; 'pat-monosomy' means that the paternal chromosome is retained in the cell (the maternal chromosome is missing); 'pat-segmentalUPD' refers to a segmental uniparental isodisomy of a paternal allele

[c] 'null' means no FISH-signals; 'del' means 1 FISH-signal; 'nor' means 2 FISH-signals; 'dup' means 3 FISH-signals. Furthermore, a second round of FISH with probes for 13qter and centromere 16 did not produce conclusive results.

[d] FISH-diagnosis is concordant with siCHILD-diagnosis, but chromosome mosaicism in the cleavage stage embryo is evident.

References

1. Van der Aa, N., Cheng, J., Mateiu, L., Zamani Esteki, M., Kumar, P., Dimitriadou, E., Vanneste, E., Moreau, Y., Vermeesch, J.R., and Voet, T. (2013). Genome-wide copy number profiling of single cells in S-phase reveals DNA-replication domains. Nucleic acids research 41, e66.

2. Vanneste, E., Voet, T., Le Caignec, C., Ampe, M., Konings, P., Melotte, C., Debrock, S., Amyere, M., Vikkula, M., Schuit, F., et al. (2009). Chromosome instability is common in human cleavage- stage embryos. Nature medicine 15, 577-583.

3. McConnell, M.J., Lindberg, M.R., Brennand, K.J., Piper, J.C., Voet, T., Cowing-Zitron, C., Shumilina, S., Lasken, R.S., Vermeesch, J.R., Hall, I.M., et al. (2013). Mosaic copy number variation in human neurons. Science 342, 632-637.

4. Ni, X., Zhuo, M., Su, Z., Duan, J., Gao, Y., Wang, Z., Zong, C., Bai, H., Chapman, A.R., Zhao, J., et al. (2013). Reproducible copy number variation patterns among single circulating tumor cells of lung cancer patients. Proceedings of the National Academy of Sciences of the United States of America 110, 21083-21088.